Saturn's Rings:
Pre-Cassini status and mission goals

J. N. Cuzzi [1] (IDS for Rings and Dust), J. E. Colwell and L. W. Esposito (UVIS), C. C. Porco and C. D. Murray (ISS), P. D. Nicholson (VIMS), L. Spilker (CIRS), E. A. Marouf, R. C. French, and N. Rappaport (RSS), and D. Muhleman (RADAR)

August 6, 2001

Abstract

Theoretical and observational progress in studies of Saturn's ring system since the mid-1980s is reviewed, focussing on advances in configuration and dynamics, composition and size distribution, dust and meteoroids, interactions of the rings with the planet and the magnetosphere, and relationships between the rings and various satellites. The Cassini instrument suite of greatest relevance to ring studies is also sumamrized, emphasizing how the individual instruments might work together to solve outstanding problems. The Cassini tour is described from the standpoint of ring studies, and major ring science goals are summarized.

1 Introduction and Overview

In November 1980, and again in August 1981, identical Voyager spacecraft flew through the Saturn system, changing forever the way we think about planetary rings. Although Saturn's rings had been the only known ring system for three centuries, a ring system around Uranus had been discovered by stellar occultations from Earth in 1977, and the nearly transparent ring of Jupiter was imaged by Voyager in 1979 (the presence of material there had been inferred from charged particle experiments on Pioneer 10 and 11 several years earlier). While Saturn had thus temporarily lost its uniqueness as having the only ring system, with Voyager it handily recaptured the role of having the most fascinating one (figure 1).

The Voyager breakthroughs (through 1984, when a series of review chapters appeared) included spiral density and bending waves such as cause galactic structure (figure 2a); ubiquitous fine-scale radial "irregular" structure, with the appearance of record-grooves (figure 2b); complex, azimuthally variable ring structure; empty gaps in the rings (figure 2c), some containing very regular, sharp-edged, elliptical rings and at least one containing both a small moonlet and incomplete arcs of dusty material; shadowy "spokes" that flicker across the main rings (figure 3); and regional and local variations in particle color (figure 4). One of the paradigm shifts of this period was the realization that many aspects of planetary rings, and even the ring systems themselves, could be "recent" on geological timescales. These early results are reviewed and summarized in the Arizona Space Science series volumes "Saturn" (Gehrels and Matthews 1984) and "Planetary Rings" (Greenberg and Brahic 1984), in Brahic (1984), and by Cuzzi (1983). An excellent review of ring dynamics at a formative stage is by Goldreich and Tremaine (1982). The reader is referred to these review articles for an introduction to overall ring properties and physics. Table 1 summarizes nominal ring dimensions and properties.

[1] Mail Stop 245-3, Ames Research Center, Moffett Field, California; jcuzzi@mail.arc.nasa.gov

From the mid 1980's to the time of this writing, progress has been steady, while at a less heady pace, and some of the novel ring properties revealed by Voyager 1 and 2 are beginning to be better understood. It is clearly impossible to cite, much less review, every advance over the last decade; however, below we summarize the main advances in understanding of Saturn's rings since the mid 1980's, in the context of the Cassini Science Objectives as described in the Announcement of Opportunity. Other review articles during this time period include Borderies (1989), Porco (1990), Nicholson and Dones (1991), Araki (1991a), Esposito (1993), Colwell (1994), Cuzzi (1995), Porco (1995), Horn (1997), Dones (1997,1998), and Burns (1999).

2 New observations

Groundbased stellar occultations detected "arcs" of ring material orbiting Neptune, starting in 1984 (see Nicholson et al. 1995 and Porco et al. 1995 for review and discussion). This suggested the need for dynamical mechanisms of azimuthal confinement of ring material in addition to radial confinement (as in the Uranian rings).

The Voyager Uranus and Neptune encounters occurred in 1986 and 1989, respectively (Science 233, 1-132; Science 246, 1361-1532; Uranus and Neptune ring systems reviewed by French et al. 1991, Esposito et al. 1991, and Porco et al 1995). The Neptunian ring arcs were confirmed. Both of these ring systems were found to be composed of a series of narrow, dusty rings embedded in a broader, very low density, more diffusely structured, sheet of tiny dust particles. The ring material is darker, in both cases, than that comprising Saturn's rings. (Ockert et al. 1987, Ferrari and Brahic 1994, Karkoschka 1997). In both systems, families of ringmoons were discovered, including several lying within the nominal "Roche zone" of the parent planet.

In 1989, Saturn's rings occulted a very bright (albeit rather large - 20 km apparent diameter) star, 28 Sagitarii (Hubbard et al. 1993, French et al. 1993, Harrington et al. 1993). In addition, several stellar occultations were observed by HST, with complex trajectories that potentially contain information about azimuthal as well as radial ring structure (Elliot et al. 1993).

The ring plane crossings of the Earth and Sun in 1995 and 1996 provided important new insights into the time-variable structure of the F ring clumps and the properties of the G ring particles, and revealed anomalous orbital behavior of the nearby moons Prometheus and Pandora (see section 3.5).

An extended series of HST color observations of the rings, as they open up, is underway at the time of this writing (French et al. 1998a, Cuzzi et al 2000). Spokes were observed in these images, and the spoke particle size determined (French et al. 1998a). The ring color was also determined in 8 filters, from the near-UV at 0.25 micron extending out to 1 micron - a great improvement over the Voyager dataset (although at lower spatial resolution). Earlier HST data, obtained with the aberration-uncorrected WF/PC, have been analyzed by Poulet et al. (1999).

Galileo has returned several new images of the Jupiter ring, which show structure not seen in the Voyager images. Amongst other results, these new data confirm the tiny nearby ringmoons Metis and Adrastea as sources of main ring material, as well as establishing

Amalthea as the parent of the gossamer ring and Thebe as a parent of an even less obvious ring (Ockert-Bell et al. 1999, Burns et al. 1999, de Pater et al. 1999). In addition, NIMS data imply that the particle size distribution is considerably steeper (richer in small particles) than previously believed (McMuldroch et al. 2000).

The Planetary Data System Discipline Node for Planetary Rings was established and has become a repository for a large amount of archival information on ring systems, including that noted above (Showalter et al. 1996; http://ringside.arc.nasa.gov).

3 Cassini ring science objectives

The science objectives of Cassini are briefly described below. Recent advances since the mid-1980's are noted, and key outstanding problems are summarized.

3.1 Configuration and dynamics

One of the most important questions about the rings is the cause of their abundant, complex structure. The "record groove" structure in the A and B rings, the hauntingly regular banded structure in the C ring, and the "kinks" in the F ring, remain unexplained.

Spiral density waves: Several studies were completed concerning the propagation and damping of spiral density waves (Shu et al. 1985, Borderies et al 1986). The different appearance of waves in the B and A ring may be understood in terms of differing particle random velocities and elasticities (Shu et al. 1985). Many weak spiral density and/or bending waves were discovered in the Voyager Radio Science data and analyzed in detail (Marouf et al., 1986, Gresh et al. 1986, Rosen et al. 1991a,b). An outstanding problem is the lack of a full treatment of coupled spiral density wave propagation, damping, and "dredging" or transport of material by angular momentum transport (Shu et al. 1985). The dredging issue has been touched on by Molnar and Dunn (1995), and the most recent attempts at wave damping and particle random velocities (ring thickness) are by Rosen and Lissauer (1988) and Chakrabarti (1989).

Irregular structure: The fine-scale radial brightness variations in the A and B rings (figure 2b) are not compatible with simple scattering models in which particle volume density is low; in fact they might indicate spatially variable particle volume density (Dones et al. 1989, 1993). The traditional way of constraining particle volume density is through the "opposition effect" of the rings, a sharp brightening within a degree or so of zero phase angle (see French et al 1998b for recent results and references). However, alternate explanations exist related to the porosity of the surface layers of each ring particle (Mishchenko and Dlugach 1992, Hapke 1990, Hapke and Blewett 1991 - see also section 4.1). Changes in volume density are expected from collisional dynamics: i.e., high optical depth regions, where the particles collide more frequently, probably have smaller random velocities and therefore smaller ring thicknesses than low optical depth regions for the same degree of stirring by large particles. In the outer 1000 km of the B ring lies a unique region where the radial structure is not only variable with longitude, phase angle, and/or time (Smith et al. 1982), but also much finer scale than seen elsewhere (Horn and Cuzzi 1996, Cuzzi et al. 1984). No satisfactory explanation exists for the irregular structure, although various local transport processes and forces have

been proposed. The most viable hypotheses include moonlet perturbations (Lissauer et al. 1981), "viscous overstabilities" (Borderies et al. 1985, Longaretti and Rappaport 1995), and ballistic transport (Durisen et al. 1992); advances in understanding these key processes continue to be of great interest. More laboratory study of the properties of impact ejecta would also be valuable (eg., Arakawa and Higa 1996).

Isolated ringlets: Narrow isolated ringlets are seen in the C ring and Cassini Division (figure 2c) - in fact in all ring systems - with a wide range of properties. We now understand how the sharp edges of the Uranian epsilon ring, at least, are maintained or "shepherded" by individual resonances due to external satellites (Porco and Goldreich 1987, Goldreich and Porco 1987). Other narrow, eccentric ringlets, such as the other Uranian rings, are becoming more well understood as "modes" in which momentum transport and the accompanying energy dissipation can reach equilibrium when the particle streamlines are arranged in a certain way (Borderies et al. 1985; reviewed by French et al. 1991 and Porco 1990). The effects of resonances on initiating narrow structures have been explored numerically by Hänninen (1993) and Hänninen and Salo (1992, 1994, 1995), and analytically by Rappaport (1998). The roles of viscosity and self gravity in maintaining these structures continue to be discussed, as improved analytical and numerical models are developed; Longaretti and Rappaport (1995) discuss the role of "viscous overstabilities" in forming narrow, eccentric rings, finding that this process cannot form an eccentric ring from a circular one. Mosqueira et al. (1999) have developed and applied a scaling approach to the dynamics, and used a smooth-particle-hydrodynamics (SPH) code to increase the range of global numerical simulations of collective effects in dense rings. Other studies along the lines of "slow" instabilities in dense rings have been done by Osterbart and Willerding (1995) and Schmit and Tscharnuter (1995). The stranded F ring, as well as the discontinuous and kinky Encke gap ringlets, probably result from different physics (discussed in section 3.5).

Ring arcs: Following the discovery of azimuthal structure in the Neptunian system, hypotheses were advanced to explain satellite perturbations which could lead to azimuthal structuring or confinement of ring material, in addition to the radial confinement previously studied for narrow rings. The essential physics of these is creation of azimuthally variable potential energy minima and maxima in the frame rotating with the ring material, about which material can then librate as do Jupiter's Trojan asteroids (Lissauer 1985). The preferred hypothesis until recently (Goldreich et al. 1986, Porco 1991) relies on corotational resonances with a moon which has a slightly inclined orbit (see Porco et al. 1995 for a review). However, more recent observations covering a longer time baseline (Terrile et al. 1998, Roddier et al. 1998, Sicardy et al. 1999, Dumas et al. 1999) have shown that the arcs have a slightly different mean motion than is consistent with the most promising confining resonance (Porco 1991). Fortya and Sicardy (1996) and Hänninen and Porco (1997) have shown that particles can escape corotational trapping and can either escape the arcs entirely or find their way to adjacent sites, compatible with a hypothesis that the arc material may be created by a disruption event and evolve, even if slowly (Esposito et al. 1997). Hänninen and Porco (1997) have also illustrated the importance of nearby vertical resonances in minimizing the collision rate among arc particles and enhancing stability, and Salo and Hänninen (1998) studied the role of self gravity of the arc material. These new insights will be valuable in understanding the properties of azimuthally variable narrow rings that Voyager actually discovered first in Saturn's rings (in the Encke gap, the Cassini Division, and the F ring

region).

Viscosity: The primary mechanism for transferring angular momentum within and throughout Saturn's rings is viscosity in the presence of Keplerian shear. The ring viscosity is a combination of random particle motions, as in classical kinetic theory, and collisions. Ring viscosity has now been modeled with allowance for finite particle sizes, close packing of particles, and the effects of mutual self gravity (Wisdom and Tremaine 1988, Mosqueira 1996, Mosqueira et al. 1999). A substantial contribution arises due to collisions between finite size particles in regions of large optical depth, causing a monotonic increase in viscosity with optical depth. This prevents the simple viscous instability (Lin and Bodenheimer 1981, Ward 1981) which had been envisioned for a system in which the viscosity has a local maximum at some intermediate optical depth (reviewed by Porco 1995 and Cuzzi 1995). Improved analysis of ring particle size and vertical structure from the Voyager radio science observations (Zebker et al. 1985) implies that the vertical thickness of the rings is only a few times the size of the larger (several meter radius) particles, which sets the velocity dispersion of the ring particles (less than 1 cm/s).

Meteoroid bombardment: The role of meteoroid bombardment in determining the structure, composition, and evolution of (at least parts of) Saturn's rings has been extensively developed in the last decade (Ip 1983; Morfill et al. 1983; Durisen 1984, Durisen et al. 1989, 1992, 1996; Lissauer 1984). The vast surface area of the rings, relative to their mass, makes them highly sensitive to meteoroid bombardment. The above papers by Durisen and coworkers propose that the morphology seen at the inner edges of both the A and B rings, involving an abrupt inner edge, a linear ramp, and several plateaus nearby, and perhaps even some irregular structure on the high-optical depth side, might result from the special kind of "ballistic transport" of ejecta associated with meteoroid bombardment. Meteoroid bombardment may also play a role in ring composition (section 3.2), in producing sporadic F ring clumps (section 3.5), and in spoke formation (see below).

Electromagnetic influences: A series of studies has suggested that magneto-gravitational instabilities favor loss of material from various parts of the rings to the planet (Northrop and Hill 1982, 1983; see reviews by Grün et al. 1984a and Connerney 1986). At least one of these "special" boundaries corresponds to otherwise unexplained changes in ring spatial structure and scattering properties (see, *e.g.*, Horn and Cuzzi 1996). The role of electromagnetic perturbations on tiny, charged dust grains was elucidated and applied to the structure of Jupiter's ring (Schaffer and Burns 1987, 1992; Burns et al. 1985, Horanyi and Cravens 1996) and Saturn's main rings (Goertz et al 1986).

"Spokes" (figure 3; Grün et al. 1984b, 1992) are believed to result from a combination of impact and electromagnetic phenomena (Goertz and Morfill 1983, Goertz 1984). The electromagnetic aspects have been further elucidated (Tagger et al. 1991) and the properties of the spoke particles better constrained (Doyle and Grün 1990). There is a clear connection, as yet unexplained, between the spokes and Saturn's planetary magnetic field; maximum spoke abundance and activity is correlated with the longitude of an active Kilometric Radiation source (Porco and Danielson 1982, 1984; also see Cuzzi et al. 1984). The role of meteoroid impacts has also been further studied by Cuzzi and Durisen (1990), who suggested that there might be a variation of spoke abundance with orbital season, depending perhaps on the ring orientation to incoming projectiles. While there has been no mention of spokes in HST images at large ring opening angles, spoke activity has now been observed from HST

at low opening angles (French et al. 1998a).

Studies were conducted of the processes by which ring material absorbs magnetospheric particles, as part of several "Ring Hazard" studies carried out under the auspices of the Cassini Project (see also section 3.4). These studies (Ring Hazard Working Group 1991, 1996) treat simultaneous absorption and diffusion of magnetospheric species, and combine imaging, magnetospheric, and spacecraft dust impact data sets into a fairly coherent picture of the faint material populating the ring plane. These results were used to constrain the ring plane crossing strategy for the spacecraft and, while not published in the open literature, are useful and available through the Cassini project or the Rings PDS Node. Canup and Esposito (1997) and Burns and Gladman (1998) present portions of the Ring Hazard Study results that constrain the ring plane crossing strategy.

3.2 Composition and size distribution

For decades, it has been known that water ice is likely to be the principal constituent of Saturn's rings. However, the known variations in color and albedo across the main rings require the presence of other constituents, in amounts that vary with location. Reviews of ring composition are in Esposito et al. (1984) and Dones (1997).

Ices, silicates, organics? Photometric analysis of the A, B, and C rings, with some interpretation as to the nature of the ring particle surfaces and vertical ring structure, has been presented by Doyle et al. (1989), Cooke (1991), and Dones et al. (1993). Data presented by Clark (1980) and Karkoschka (1994) might show a very weak 0.85 micron absorption feature (see also Clark et al. 1986). Estrada and Cuzzi (1996; EC96) analyzed the radial variation of color across the main rings in three Voyager (visual) wavelengths; unfortunately the plots in EC96 contained incorrect calibration constants. The revised ring colors (figure 4, retaining the Voyager "atmospheric" calibration discussed by EC96) are less red. Doyle et al. (1989) constrain the abundance of non-icy material from visual wavelength data; Cuzzi and Estrada (1998) extend and refine this analysis, and incorporate it with an evolutionary model which shows how meteoroid bombardment causes the color and composition of the rings to evolve with time.

Both Doyle et al. (1989) and Cuzzi and Estrada (1998) conclude that observed ring particle compositions are not compatible with exposure to current estimates of interplanetary debris over the age of the solar system. Cuzzi and Estrada (1998) infer from the observed ring properties that the reddening agent is more likely to be an "intrinsic" organic tholin-like material than a silicate. The darkening material is most likely "extrinsic", dark, neutrally colored carbonaceous material. Results from new HST data (Cuzzi et al 2000) reveal an unexpected increase of ring redness with phase angle (not tilt angle), which is larger than is seen for, at least, Europa (Helfenstein et al. 1998) and invalidates the interpretation of the Voyager G/UV ratio by Cuzzi and Estrada (1998) as purely an albedo effect. The newly calibrated Voyager results (figure 4) are compatible with this effect. However, a new analysis for the ring particle albedo and composition now needs to be done including data over a range of phase angles. The new HST results include evidence for regional variation of composition from several new passbands - 255nm and 1042nm. Color ratio profiles imply the presence of different materials responsible for absorption at these and other wavelengths with rather different radial distributions.

Microwave emission is highly sensitive to small amounts of non-icy material spread uniformly throughout the ring particles. Epstein et al. (1984) limited the abundance of silicates to 10% by mass; recent studies by Grossman (1991; see also Grossman et al. 1989) indicate the non-icy material fraction might be even lower - perhaps as low as 1%. Even more recent observations confirm these low ring brightnesses and the cause as scattering of Saturn's thermal emission and the cold of space (de Pater and Dickel 1991, Molnar et al. 1998, van der Tak et al. 1998) and seem to agree on a weak East-West asymmetry in the ring brightness. The cause of this is not known at present, but might be related to the same trailing wake structures advocated to explain similar effects at visual wavelengths (*e.g.*, Colombo et al. 1976, Dones et al. 1993). The usual framework for interpreting microwave observations, including radar reflectivity, is a more-or-less classical scattering layer (modified to account for finite thickness; Cuzzi et al 1980, Zebker et al 1985). However, recent suggestions that some of the large radar reflectivity of the Galilean satellites might be due to a coherent backscatter opposition effect (Mishchenko and Dlugach 1992, Hapke 1990, Hapke and Blewett 1991) might merit more consideration in the ring radar context as well.

Photometry of the D ring (Showalter 1996, Marley and Porco (1993)), E ring (Showalter et al. 1991), F ring (Showalter et al. 1992), and G ring (Showalter and Cuzzi 1993, Throop and Esposito 1998) is discussed further below.

Particle size distribution: A new approach to analysis of stellar occultation data was developed that provides good constraints on the size of the largest local particles at very high spatial resolution (Showalter and Nicholson 1990). Fluctuations in the brightness of an occulted star are observed that are above the levels predicted by Poisson statistics; these are interpreted in terms of uneven filling of the star's Fresnel zone (about 20 m on a side) by objects at the large size end of the particle size distribution. Interesting comparisons can be made between these results and more direct measurements of "largest" typical particle size, such as from Voyager radio occultations (Tyler et al. 1983, Marouf et al. 1983, Zebker et al. 1985). Agreement is not always as good as might be hoped, and improvements in the technique are probably indicated, but it shows how stellar occultation experiments can complement radio occultation measurements, providing high spatial resolution information on the abundance and size of the largest particles. More recent analysis of the 28 Sagitarii occultation constrains the lower end of the size distribution; the B ring particles are larger than 30 cm, while the size distribution extends further into the cm-size range in the other rings (Nicholson and French 1998). In the Cassini era, given a fuller understanding of the polarizing properties of irregular particles, currently puzzling polarization observations (Dollfus 1996) might become better understood.

The evolution of particles and clumps of particles by collisional sticking and growth, with spins and tidal and/or collisional disruption, has been studied analytically (Araki 1988, 1991b; Longaretti 1989). Laboratory studies have been done which constrain the plausible range of ice particle stickiness at low relative velocities for a variety of surface conditions (Bridges et al. 1996, Supulver et al. 1997, Higa et al. 1996). Numerical simulations of combinations of dynamical and collisional behavior of rings (and more general N-body systems) which include realistic inelasticities have shown the formation of transient clumps (Salo 1991, 1992a,b, 1995; Richardson 1994). These large structures are reminiscent of the "dynamical ephemeral bodies" postulated for the 5-10 meter-sized ring particles themselves by Davis et al. (1984). The large fluctuations observed in stellar occultation data (Showalter and

Nicholson 1990) might be related to these structures. More quantitative discussion of their relative abundance will be needed before we can determine if such structures are significant contributors to remote observations of "particle size" from radio or stellar occultations.

Diffuse rings and tiny grains: The E ring is now fairly well understood as dominated by micron-sized grains, based on a large number of complementary groundbased and spacecraft observations (Burns et al. 1984, Showalter et al. 1991); especially diagnostic are its blue color and vertically extended spatial distribution (discussed further in section 3.4).

Recent observations and modeling studies of the G ring (Throop and Esposito 1998, Meyer-Vernet et al. 1998, Nicholson et al. 1996) have revised our beliefs regarding the size and radial distribution of material in that region. Van Allen (1983) had concluded that the radial width of macroscopic material (capable of absorbing magnetospheric protons) was only around 500 km; Showalter and Cuzzi (1993) had reconciled this with Voyager images which clearly show a much broader feature by suggesting that the visible 5000 km wide ring is merely a broad dusting of tiny grains surrounding a narrower core of large objects. Showalter and Cuzzi (1993) also concluded from the (admittedly sparse) phase angle distribution of Voyager images that the diffuse Voyager G ring probably contained dust with a very steep (r^{-6}) size distribution. The newer results and analyses change these beliefs as follows: (a) the G ring material is confined to a relatively narrow vertical layer across its entire radial extent, as opposed to the obviously vertically extended E ring (Nicholson et al. 1996), (b) the G ring material is red-to-neutral in color, as opposed to the distinctly bluish hue of the E ring (Throop and Esposito 1998), and (c) reanalysis of Voyager PRA data showing impacts on the Voyager 2 spacecraft as it traversed the periphery of the G ring (Meyer-Vernet et al. 1998) are incompatible with the steep size distribution and dominance by tiny, submicron grains found by Showalter and Cuzzi (1993). Since several lines of argument find the E ring to be composed primarily of micron-sized particles (section 3.4), these results suggest that the G ring is *not* similarly composed, and that macroscopic material permeates the entire radial width of the G ring (which may still be compatible with the analysis of Van Allen 1983). The recent conclusions are all compatible with a distributed moonlet belt model covering the entire width of the G ring (Canup and Esposito 1997), doubtlessly coexisting with a complement of tiny dust grains as seen in Voyager images.

3.3 Dust and meteoroids; local and interplanetary

The influence of meteoroid bombardment on ring structure and composition has been discussed above in several places. While important uncertainties will require resolution by Cassini, especially in regard to the net flux and composition of the projectiles, some progress is being made. A collection of the different data sources, with a non-physical interpretation in terms of dynamical populations, was presented by Divine (1993). The Galileo and Ulysses missions have measured the abundance of tiny grains in the outer solar system (see, e.g. Grün et al. 1997 and references therein).

Recent observations of water in the stratospheres of Saturn and the other gas giants, interpreted with the aid of model photochemical calculations, place interesting constraints on the meteoroid mass flux (Feuchtgruber et al. 1997, Moses 1998, Moses et al. 1998). The (one-sided) mass flux implied is compatible with a recent reassessment by Cuzzi and Estrada (1998): about 5×10^{-17} g cm^{-2} sec^{-1} prior to gravitational focussing by the planet. Galileo

and Ulysses have found a population of plausibly interstellar grains (Grün et al. 1997); Dones (1997) suspects the mass flux at Saturn (as inferred from Pioneer) could be considerably lower - if the interstellar grains contain larger members than commonly assumed, their impact velocity on the Pioneer dust sensors is sufficiently higher than that of ambient projectiles to offset their smaller masses. Cuzzi and Estrada (1998), on the other hand, believe that these grains are probably too small and too few to significantly affect the mass flux into the rings, which is dominated by much larger (100 micron radius) objects. Showalter (1998) obtains a constraint on cm-sized particles in fair agreement with these fluxes. Overall, the mass and velocity distribution of the dominant projectiles at Saturn are key goals for the Cassini CDA; the velocity distribution affects the gravitational focussing and longitudinal impact distribution, and the mass and composition will limit the ring age (Doyle et al. 1989, Cuzzi and Estrada 1998; see sections 3.2 and 4.1).

3.4 Ring-atmosphere/ionosphere/magnetosphere interactions

The outer, diffuse E, F, and G rings interact with Saturn's magnetosphere, and the main rings interact with Saturn's ionosphere as well as, perhaps, its atmosphere. The structure and particle properties of Saturn's E ring (section 3.2) make a clear case for a particular combination of meteoroid ejecta, solar radiation pressure, and charged particle dynamics in producing this unique structure (Horanyi et al. 1992; Hamilton and Burns 1993a, 1994). Essentially, particles of size narrowly localized to one micron radius, orbiting in the magnetosphere, attain a charge-to-mass ratio just sufficient for Lorentz forces to cancel out their orbital precession rate. The orbital eccentricities of this narrow range of particle sizes are then pumped to high values by solar radiation. The E ring does seem to have a particle size distribution narrowly confined to just this size range, based primarily on its blue color (Showalter et al. 1991). This model would predict at least *some* similarly diffuse rings associated with the other icy moons (A. Cheng, personal communication, 1996), and in fact there does seem to be an unmodeled component just interior to the orbit of Tethys (Showalter et al 1991).

Radial variations in the abundance of various magnetospheric species have been used to constrain several properties of ring regions, because tiny amounts of ring material can produce noticeable depletions of rapidly mirroring charged particles (Van Allen 1983, 1984; Cuzzi and Burns 1988, and two ring hazard studies available through the Cassini project). A new model of *microsignatures* (longitudinally confined, radially narrow depletions) and *macrosignatures* (axisymmetric, radially broad depletions) has been presented by Paranicas and Cheng (1997). Evidence for longitudinally variable material in the E ring region remains controversial (see Van Allen 1984 for a discussion of the charged particle data, and Roddier et al 1998b for a puzzling visual detection of an "arc" in adaptive optics data). Key uncertainties in interpreting microsignatures in terms of absorbing material include the poorly known identity and diffusion coefficients of the relevant magnetospheric species, and these will be important goals for Cassini MAPS.

A connection has been demonstrated between the rings and the atmosphere/ionosphere of Saturn, in that water vapor ejected from the rings by meteoroid bombardment impinges on the planetary stratosphere and ionosphere, with dramatic effects on electron density. The abundance of this water can, in principle, be used to constrain the meteoroid flux and loss of

matter from the rings (Connerney and Waite 1984). Preliminary results have been reported for a direct observation of elevated water abundance in latitudes connected to the rings, which is compatible with a large water mass loss rate (Fouchet et al. 1996); however, the transport process, and the chemistry and loss processes within the stratosphere, are highly complex and need to be modeled carefully before implications can be drawn about water mass loss from the rings (*e.g.* Moses 1998, Moses et al. 1998). Recent HST observations of the "atmosphere" of the rings (Hall et al. 1996) support earlier inferences of about 600 - 700 atoms cm^{-3} (reviewed by Cuzzi et al. 1984) and provide some support for commonly assumed meteoroid flux values. Estimates by Ip (1995a) had been much lower. Ip (1995b) also estimated the visibility of ejecta during the 1995-1996 ring plane crossings, but no attempt has yet been made to compare these with the observations.

3.5 Ring-satellite relationships; ring origin/evolution

The origin and evolution of ring systems is so closely connected to "ring-satellite relationships" that we merge these two Cassini science goals.

As described in previous sections, Saturn's main rings (as well as other ring systems) are significantly evolved in composition and structure. On geological timescales, it has long been believed that dynamical evolution of the rings under moonlet torques removes both the rings and the inner ringmoons from their current locations in times much shorter than the age of the solar system (Goldreich and Tremaine 1982, Lissauer et al. 1985, Esposito 1986). As also discussed above, it has more recently been realized that meteoroid bombardment will alter the ring structure and composition on comparably short timescales. Ip (1984), Lissauer (1984) and Cuzzi and Durisen (1990) show that angular momentum dilution by infalling material can be important in causing orbits of ring material to decay. While both the dynamical and the meteoroid effects have their uncertainties, they independently point in the same direction. The general problem of "short timescales" in planetary rings, and specifically in Saturn's rings, was recently reviewed by Cuzzi (1995) and by Dones (1997), who differ on the robustness of the arguments for a recent origin of Saturn's rings (see section 3.3). To infer ring origin, we must peer back through all this evolution and time variation.

Many of the issues of ring origin and evolution are closely linked to the existence of nearby "ringmoons" - 1-100 km sized bodies which dynamically interact with the rings and/or provide source material to replace mass rapidly lost in small particles. It is now clear that the four gas giants are surrounded by systems in which rings and moons are intermingled; this is illustrated in figure 5 (Nicholson and Dones 1991). The moonlet Pan was inferred and subsequently discovered orbiting within the Encke gap in Saturn's A ring (Cuzzi and Scargle 1985, Showalter et al. 1986, Showalter 1991, Horn et al 1996), where two radially distinct "ring arcs" are also to be found (Ferrari and Brahic 1997). Gap-embedded moonlets have also been inferred in the Cassini division based on what appear to be "wakes" (Marouf and Tyler 1986) but imaging analysis of the region casts doubt on the "wake" interpretation (Flynn and Cuzzi 1989) and the moonlet inference; the cause remains one of the many unsolved problems of Saturn's ring structure.

The inner ringmoons of Saturn (including the probably misnamed "F ring shepherds" Prometheus and Pandora, and the coorbital satellites Janus and Epimetheus) seem to have unusually low internal densities - 0.3 to 0.6 g cm^{-3} (Rosen et al. 1991b, Yoder et al. 1989,

Nicholson et al. 1992). HST observations, starting in the 1995-1996 ringplane crossing epoch have revealed anomalous dynamical behavior for both Pandora and Prometheus (de Pater et al. 1996, Nicholson et al. 1996, Bosh and Rivkin 1996, Bauer et al. 1997, French et al 1999). An irregularly increasing lag in the longitude of Prometheus from that predicted from Voyager orbital elements (Bosh and Rivkin 1996, Nicholson et al. 1996) might be explained by an encounter of Prometheus with a moonlet buried within the F ring as their orbits precess to an intersecting configuration (Murray and Giuliatti-Winter 1996). The Pandora orbital changes might be due to a nearby resonance with Mimas (French et al. 1999). It is clear that the dynamics of the region is more complex than previously believed.

The collisional and dynamical evolution of "moonlet belts", in which visible dust grains are generated by mutual collisions between and extrinsic bombardment of large, possibly unseen, parent bodies, while sweepup and even reaccretion continuously operate, has been studied in a series of papers aimed at the F ring region of Saturn (Cuzzi and Burns 1988, Poulet et al. 1998), as well as at the ring-moon systems of Uranus and Neptune (Colwell and Esposito 1992, 1993). Early work along these lines had been done in the Jupiter ring context by Burns et al. (1980). Models have also been applied to Saturn's G ring (Showalter and Cuzzi 1993, Canup and Esposito 1997). The recent G ring results of Throop and Esposito (1998) are compatible with a moonlet belt hypothesis. Canup and Esposito (1995) modeled the accretion of objects closer to the planet, even inside the Roche limit.

The F ring will provide Cassini with perhaps its best example of a dynamically evolving ringmoon belt. There have been theoretical and observational studies of the current F ring strands (Lissauer and Peale 1986, Murray et al. 1997). Furthermore, the F ring is now known to be highly time variable, in that bright clumps in the ring come and go on a range of timescales (Showalter 1998). Specifically, the several bright "knots" seen by Voyager 1 do not correlate with those seen by Voyager 2, and one bright region in a series of Voyager 2 frames is seen to generate new clumps on a daily timescale, which move at different orbital rates from the main clump which generates them (Showalter 1998, Bosh and Rivkin 1996, Nicholson et al. 1996). Showalter (1998) suggests that some of these clumps form by extrinsic impacts into the F ring; Poulet et al. (1998) suggest that others form by collisions between large F ring objects. Cuzzi and Burns (1988) proposed that microsignatures seen near, but not in, the F ring may be transient debris generated by collisions between unseen members of a moonlet belt surrounding the rings, which could be stirred by perturbations from Pandora and Prometheus (Scargle et al. 1993), and that the F ring itself may be a recent, unusually large, collisional product. Intriguing clues do exist for uncatalogued objects lying outside of the F ring itself but in the general region of potential interaction (Kolvoord et al 1990, Harrington et al. 1993, Gordon et al. 1996). A difficulty with this concept is the apparent lack of the fine dust one would expect to be associated with such collisionally generated debris (Showalter, personal communication, 1998). Clearly, there is considerable "action" awaiting Cassini in this regard (see also Borderies 1992).

constraints on ring origin? Theoretical estimates of the lifetimes of moons and moonlets in and around ring systems indicate their lifetimes are shorter than the age of the solar system (Colwell and Esposito 1992, 1993); thus ongoing creation of narrow rings and ringlets, such as in the Uranian and Neptunian systems, or the G ring of Saturn, could readily follow occasional disruption of parent moonlets. This concept was first discussed by Harris (1984). Specific application to the disruption lifetimes of the inner moons of Saturn was presented

by Lissauer et al. (1988). Saturn's rings continue to present a hurdle for recent creation, due to their very large mass (about the mass of Mimas). Lissauer et al. (1988) estimate from crater abundances that the likelihood of disrupting a Mimas-size precursor in the last 10^8 years is rather small - about a percent.

Alternatively, Dones (1991) reconsidered the plausibility of tidal (classical Roche style) breakup of a heliocentric object, and retention of some fraction of the debris (a scenario similar in some ways to comet Shoemaker-Levy's recent encounter with Jupiter), and found a probability comparable to that of impact disruption (or perhaps higher if S/L9-like cases are considered (Dones, personal communication, 1999). Cuzzi and Estrada (1998) suggested that the color/compositional properties of the rings differ from those of the Saturnian moons, and resemble those of Triton more closely; they suggested that this favors tidal breakup of an extrinsic, heliocentric object rather than impact disruption of a native-born resident of the system. However, in view of the revised ring colors emerging from reanalysis of the original Estrada and Cuzzi (1996) results (section 3.2), this conclusion will need to be revisited. Additional research into the fragmentation of realistic bodies on realistic trajectories would certainly be welcome.

4 Instrumental approach

Details of the science investigations are described in the individual papers by the instrument teams. Below we present high-level introductions to the main contributions of the different instruments to ring science objectives.

The UltraViolet Imaging Spectrometer (UVIS) will provide spectral images of the rings, constraining the location and distribution of water ice *vs.* other materials; a strong absorption edge shown by water ice will be prominent in the properties which will be studied. Because it has the shortest wavelength, UVIS images will be sensitive to the smallest dust particles. UVIS will also measure H,D, and O to characterize ring evolution, water loss, ring atmosphere, history, and current ring-magnetoshere interactions. Perhaps the primary contribution of UVIS to ring science will be its stellar occultation capability. Observing stellar occultations in the UV greatly reduces ring background, since the rings are extremely absorbing in the UV; the Voyager stellar occultation (of the UV star δ Scorpio) provided the highest spatial resolution of any instrument (the Fresnel zone on the rings was only tens of meters across). For δ Sco, Cassini UVIS has 50 times the sensitivity of the Voyager PPS with 5 times smaller resolution. Two kinds of information are derived from these data: highly detailed, fine resolution scans of the optical depth of ring material, including our best observations of spiral density waves and sharp ring edges, *and* constraints on the radial variation of the abundance of *large* ring particles (those with size comparable to the Fresnel zone; Showalter and Nicholson 1990).

The Imaging Science System (ISS) is the highest resolution two-dimensional imager on the Orbiter and will provide unique information on variation of structure with radius, azimuth, and time; the ISS Narrow Angle Camera (NAC) and its Wide Angle Camera (WAC) have typical resolution of 6 and 60 microradians, respectively. The ISS cameras are far more sensitive than the Voyager cameras, and one expects many small moonlets will be discovered in gaps within the rings, and perhaps outside the rings in and around the F and G ring

regions. Furthermore, the ISS has the unique ability to cover a very broad range of azimuth in one observation. Greatly improved dynamical models will result from the high accuracy observations of mean motion, inclination, and eccentricity of ringmoons. Images in multiple filter bands will provide good constraints on ring particle composition with excellent spatial resolution. Variability of ring brightness with observing geometry (phase angle, illumination angle or solar elevation angle, and viewing elevation angle) will constrain the local volume density of the rings, and thus the local dynamics and viscosity. Highly sensitive detection of tiny amounts of microscopic dust at high phase angles will map out regions of active collisional evolution.

The Visual and Infrared Mapping Spectrometer (VIMS) will provide unique information on the detailed spectral fingerprints of different materials in the rings, from their diagnostic lattice vibration features. Distinction between icy, silicate, and perhaps even organic material will be possible. Information about ring particle regolith grain size will be obtained from the depths of different absorption features. The VIMS instrument has a 0.5 millirad (mr) pixel size and several fields of view, from the size of the NAC field of view (6 mr) to 32 mr. In addition, VIMS has created a capability for stellar occultations comparable to the capability of UVIS; observations of an entirely different stellar population (bright infrared stars) can be conducted in water ice absorption bands. The wide difference in wavelength between these occultations and the UV stellar occultations of UVIS will constrain the relative abundance of fine dust particles in the rings, which are effective at blocking UV radiation but not IR radiation.

The Composite Infrared Spectrometer (CIRS) is a Fourier transform spectrometer that measures thermal radiation from 10 to 1400 cm^{-1} (1 mm to 7μ), with a spectral resolution that can be set from 0.5 to 20 cm^{-1}. The far infrared portion of the spectrum (17μ to 1 mm) is measured using thermopile detectors which collect radiation through a 4 mr FOV. The middle infrared section is measured using two focal planes (7μ to 9μ and 9μ - 17μ) each with a 1 x 10 array of HgCdTe detectors. Each detector has a 0.3 mr FOV. Observations of the ring temperatures at thermal wavelengths (the 100K ring temperature has peak emission at 30μ wavelength), especially how they vary diurnally as a function of ring optical depth, radius, and solar elevation angle, can provide constraints on local ring dynamics (history of particles moving from lit to unlit faces of the ring). The composition and/or porosity of the regoliths of ring particles might vary with location, and these data will provide another handle on separating this variation from other effects. In addition, the millimeter channel will sense emission emerging from throughout the ring material (the absorption pathlength for millimeter emission in ice at 100K is several meters), and even small radial variations in mixing fraction of non-icy material will be mapped.

The Microwave Radiometer, part of the Radar system, will sense ring radiation at 2 cm wavelength, using the high-gain antenna with a resolution of 6.5 mr. Radiation at 2 cm wavelength contains, in addition to thermal emission, a somewhat larger component due to diffuse scattering of the planetary thermal emission than found at 1 mm wavelength, and will complement the CIRS observations. The 2 cm wavelength radiometer will sense thermal emission throughout icy particles smaller than about 5 meters.

The Radio Science Subsystem (RSS) uses multiple wavelength (0.94, 3.6, and 13 cm) occultation and bistatic-scattering observations to map ring structure and determine ring physical properties. The wavelengths are ideally matched to the centimeters-to-meters radius

distribution of ring particles, which dominate ring opacity and mass. The observations provide the unique capability of mapping the relative abundance of the 1 to 20 cm radius particles within individual ring features, as well as determination of the full size distribution and vertical thickness of broad ring features that can be resolved in the signal spectra. Multiple high-resolution optical depth profiles obtained at different viewing geometries and times will provide "tomographic" mapping of the variability of radial, azimuthal, vertical, and temporal ring structure, important for quantitative characterization of physical and dynamical processes. The larger ring opening angle, multiple occultation opportunities, and three wavelength capability will permit significant improvements over the Voyager RSS observations, particularly for the optically thick B Ring which blocked the Voyager radio signals over most of its width.

The Cosmic Dust Analyzer (CDA) will directly sense the composition of "ring" material that it encounters, such as in the E (and perhaps G) rings. It will also provide essential data on the mass flux, particle size distribution, composition, and orbital elements of interplanetary and circumplanetary projectiles that continually bombard the rings. This information is critical to unraveling the role of meteoroid bombardment in evolving the structure, composition, and even the age of the main rings, as alluded to above.

Other contributions to understanding the rings will be made by the extensive suite of particle and field experiments, as in previous missions. For example, observations of microsignatures and macrosignatures as functions of magnetospheric particle species and energy, can tell us much about the presence of clumps of debris too transparent to be observed by remote sensing instruments. Also, measurements of pulses of ionized material created when tiny particles hit the spacecraft have proven to be highly sensitive to very small amounts of tiny particles in the ring plane. These and other contributions to ring science are detailed in the papers by the respective instruments.

4.1 Examples of how instruments might be used together to solve outstanding problems:

Answering the "big questions" of, for instance, the origin and age of Saturn's rings will require combining the observations from most of the instruments on the spacecraft.

A combination of occultation and imaging data led to the discovery of the Encke gap moonlet; similarly, we expect that discovering and studying ever tinier moonlets in and around the rings will be best done by combining imaging (direct detection; indirect detection from edge waves; detection of time-variable clumps from collisions, etc) with stellar and radio occultations (detection of wakes in surrounding material - strongly variable with longitude). In a similar way, unraveling the nature of the irregular structure, including the distinction between angular and temporal variation, will require a variety of images and stellar and radio occultations at different times and longitudes.

Studies of very low optical depth moonlet and debris belts, such as the G ring and perhaps material near Lagrange points, can best be done by combining the great sensitivity of magnetospheric particles to absorption by tiny amounts of matter (as detected by the MAPS instruments) with direct deep imaging searches.

Recent work has shown that evolution of the color and composition of the rings under

meteoroid bombardment might provide a significant constraint on the origin and age of the rings. Models of the process require the radial variation of *both* ring optical depth and ring particle size variations (which, along with optical depth, determine surface mass density) with location. Particle size variations are obtained from stellar occultation fluctuations, or by comparison of optical depth from optical and radio wavelength occultations. Models of radial variation of ring composition will use color data from imaging broadband filters, reflection spectra from VIMS, and/or total thermal emission from CIRS millimeter-wave and/or centimeter-wave Radiometer data.

Ring viscosity, a critical evolutionary parameter, will be established from combining several different observations: local (radially variable) volume density measurements may be inferred from imaging the opposition effect and by comparing ring brightness over a range of phase angles. If the opposition effect indeed constrains the "packing density" of the rings, it will then constrain the particle relative velocity which is essential for understanding the fine scale structure and its local dynamics. Or, the opposition effect might simply refer to the particle surface structure as mentioned in section 3.1. It is thought that these possibilities can be distinguished by adequate coverage of the effect as a function of illlumination, viewing, and phase angles, wavelength, and possibly polarization. RSS measurements of ring optical depth at several ring tilt angles will constrain vertical ring structure, hence the relative velocities of the largest particles, which carry most of the ring mass; CIRS measurements of particle diurnal (and eclipse) heating/cooling will tell us the ease with which particles migrate vertically in the ring, another measure of ring viscosity.

Compositional evolution involves ring viscosity as constrained from multi-instrument observations. In order to convert ring evolutionary age in dimensionless units, obtained from modeling color profiles using all these data, to an actual ring age requires absolute interplanetary and circumsaturnian projectile mass fluxes and velocity distributions, which will come from CDA. CDA will also provide a better estimate of the composition of the interplanetary projectiles, a key unknown of the model.

5 Cassini Tour

The Rings working group met in July 1995 to forge a coherent set of prioritized science requirements, emphasizing those which drove tour geometry.

We categorized our requirements as Priority I (Excellent, must have), priority II (Very Good, should have), and priority III (Good, want to have). These are the same classes of priority as widely used by peer review panels. We had extensive debate across the teams as to what distinguished *must* have (uniqueness, new observational geometry, new instrument, critical resolution threshold, time baseline, etc) from *should* have (multiple wavelengths, longitudes, times), or *want to* have ("complete coverage of...", "maximum range of...", "fill in phase space of...", etc). This prioritization did provide us with a convenient way of making numerous decisions concerning tours and defending our decisions.

In the brief paragraphs below, we present a simplified version of the science requirements which drove tour geometry (the more detailed requirements are documented in project reports). From these different science needs, metrics were derived to judge the relative quality of candidate tours. Many important science goals are not specifically called out herein (see

instrument team reports), but we do mention a few supportive science goals where appropriate, or where the combination of all requirements together provides knowledge that none of them does individually (such as photometry) but the key geometries are individually justified on the grounds of unique and essential science. The requirements are in rough priority order.

5.1 "Must have" ring observing geometries for the Cassini tour

(1) Adequate time in nearly diametric Earth occultations as early in the tour as possible, with spacecraft distance approximately 5-6 Saturn radii (R_S) behind the planet. These are "dayside apoapse" revs.

This geometry simultaneously provides three of the most critical observing geometries for ring science, and is therefore one of the highest priority "must have" tour elements. Diametric Earth occultations, with the spacecraft at 5-6 R_S behind the planet, provide RSS with the required radial resolution to explore known classes of structure in both the direct and the "scattered" signals (each providing structural information for different size particles). In addition, only while the sun is occulted by Saturn can ISS obtain the unique, high resolution, very high phase angle observations which so strongly delineate clumps and kinky ringlets, as well as extremely low-optical depth dust-sized material. In these orbits, the Sun is also occulted by the rings and planet as seen from the spacecraft, providing unique information on ring composition for VIMS and UVIS. Finally, this same geometry also provides observing times when the opposition effect can be observed moving across the rings. The requirement to have these 6-7 revs as soon in the mission as possible derives from the fact that the ring opening, as seen from Earth, decreases with time, and the denser regions rapidly become impenetrable to RSS (the slant angle appears in an exponential). It is not currently known, for example, just how opaque the densest parts of the B ring are! This geometry, together with the geometry provided by (3), (4), and (5), provides an adequate range in viewing angle coverage of the rings as solar illumination angle varies from highest to lowest.

(2) Adequate time at high resolution (range $< 6R_S$), observing the lit face at low phase angle ($< 45°$) and moderate s/c latitude (45° or more). These are "nightside apoapse" revs (this requirement was subsequently bifurcated into two slightly different geometries).

High resolution, lit face, high latitude observations are critical geometries needed to address several key unknowns related to the question of the origin and evolution of the rings, which is one of the highest priority objectives for Cassini ring science. The composition of the ring material is one such key current unknown. It is known that particle composition varies from place to place and on radial scales of 50-100 km. Resolution-limited instruments (VIMS, CIRS) must be able to resolve this known structure to make required observations as to how particle composition and/or thermal properties vary; this determines the required observing distance as stated above. Detecting faint spectral features also requires high signal-to-noise observations, which are best made where the rings are brightest - on the lit face of the rings at phase angles which are less than 45° and optimally between $10 - 30°$.

The temporal evolution of observable ring structure, and the distribution and gravitational influence of embedded and external satellites, are other key current unknowns in this regard. The combination of high latitude and high resolution stated above is required for ISS to make better-than-Voyager measurements, over a range of ring orbital longitudes, of cer-

tain fine scale ring features which are known to be azimuthally and/or temporally variable; the cause of this structure is currently unknown and determining its origin and evolution is one of the highest priorities for ISS. Low phase angle observations are required so that these observations can simultaneously accomplish the science objectives of both discovering, and determining the orbital elements of, satellites in the (roughly) dozen known genuine gaps in the rings, and in studying the structure, kinematics and dynamics of gap-embedded ringlets. (Small embedded satellites are easiest to detect and observe at moderate-to-low phase angles.) High-resolution observations from high latitudes will probably be obtainable in polar orbits late in the mission, but this will only provide one of (minimally) two points needed (i) to distinguish time variation from spatial variation for ring feature observations, and (ii) to determine the rates of changes of the orbital elements of newly discovered satellites. Consequently, it is essential that there are opportunities for these geometries to occur in the early-middle part of the tour, to provide a good time baseline with "polar orbit" observations, most likely at the end of the tour.

(3): Adequate time at high inclination ($60 - 70°$ with low periapse (3-5 R_S) (which turn out to be satisfied primarily by a "Polar Orbit Sequence").

The B ring is so dense that its optical depth has never been measured over a considerable fraction of its radial extent at resolutions on which structure is known to occur. Stellar occultations by UVIS and VIMS will provide not only the ultimate in structural information but also, from detailed analysis, information about particle size distributions at both micron- and meter-scales. Only this sequence provides sufficiently numerous stellar occultation opportunities at sufficiently high signal-to-noise ratio to allow measurement of structure and particle properties in high optical depth regions at full radial resolution (20 meters). The combination of small distance from Saturn and high inclination (close proximity to the rings at high latitudes) ensures the occurrence of tens of high quality UV stellar occultation opportunities (bright O and B stars) because the rings cover a large angular extent and have a large opening angle relative to the line of sight. Our investigations of other geometries have shown that the quality of occultations available at moderate inclinations (such as the "diametric Earth occultation" sequence of element (1), or typical Titan 180° transfer orbits as described in section 5.2.2) is significantly worse for two reasons: the rings are more opaque because they are more oblique to the occultation path, and their smaller apparent size reduces the number of candidate stars. For various reasons, it appears that "polar orbits" are best situated near the end of the tour. Sunward apoapsis for the polar orbit sequence is preferred for three reasons related to ring studies. First, it allows UVIS and VIMS ring stellar occultations to occur across the rings in Saturn's shadow, which provides the lowest possible background. Second, it provides optimum viewing by CIRS (with adequate radial resolution near periapse) of the shadowed region which is most diagnostic of ring thermal properties. Third, nightside periapse provides several times better resolution for profiling ring structure using the direct component of the RSS occulted signal. Several decent, although not diametric, chords across the rings can be obtained in this geometry. Fourth, the near-polar geometry provides adequate time and resolution to enable radiometry of the rings with the 2 cm-wavelength Radar feeds. Centimeter-wavelength radiometry is the only way to penetrate the entire volume of ring material and detect "buried" materials of non-icy composition. The large Radiometer beamwidth requires close observing distances to resolve known structure of interest. This geometry, together with the geometry provided by (1), (4),

and (5), provides an adequate range in viewing angle coverage of the rings as solar illumination angle varies from highest to lowest. Finally, to the extent that this geometry provides solar occultations, ISS will be able to obtain a time baseline on temporal evolution of dusty, fine-scale structure using high phase angle observations (relative to element 1 above).

(4): A second series of 3-4 Earth occultations; ring opening angle (from Earth) of $14-18°$ with range $< 5-6R_S$ antisunward.

The driving requirement here is for RSS to obtain unique information at tilt angles between the maximally open geometry found early in the mission (bullet 1), and the nearly "edge-on" configuration in which Voyager observed them, which is approached at the end of the Cassini mission. The nominal target tilt angle here is in the range $14-18°$. The combinations of observations obtained this way will allow unique information to be inferred about ring vertical thickness and structure in all three main ring regions. It is difficult to obtain the full complement of information from RSS data if the geometry is not tuned to mitigate Doppler smearing of the scattered signal. We believe this can be alleviated by some moderate optimization of occultation tracks within opportunities obtained just before, during, or after a suitably oriented Titan 180° transfer or other inclined sequence. For example, occultation tracks can be adjusted to begin and end off the planet, and/or to cross the rings in a configuration which is roughly diametric. Also, orbital tour "tweaks" at this stage may once again allow the ring opposition effect to be observed by ISS at a different solar elevation angle, allowing much stronger constraints to be placed on ring vertical structure and distinguishing ring packing density influences from particle regolith effects.

(5): Adequate time in two widely spaced epochs (prior to mid-mission and after mid-mission) with S/C latitude $> 30-45°$, distance to rings $< 14R_S$, and phase angle $< 90°$.

This element provides the critical time baseline and coverage needed for ISS to perform orbit determination of the myriad small embedded satellites that Cassini is sure to discover and the structure they cause, amongst other goals. For instance, high accuracy in orbit determination is needed to measure the acceleration of nearby ringmoons away from the rings - a key measure of ring lifetime. It is also needed to separate moonlet orbital inclination from eccentricity - important for azimuthal confinement of "arcs". Furthermore, resolved images of small moonlets, and their orbital changes, as they gravitationally interact with other moons and ring material, will provide the only means of determining the moonlet densities. This geometry, together with the geometry characterized by (1), (3), and (4), provides an adequate range in viewing angle coverage of the rings as solar illumination angle varies from highest to lowest. Furthermore, it provides another key time point for numerous stellar occultations. Occultations in this geometry will be less numerous and generally have a lower signal to noise ratio than during the polar orbits for reasons discussed under bullet (3). However, if the distance from Saturn is larger, the occultations will be slower and thus low and moderate optical depth regions can be studied with higher sensitivity.

5.2 Brief illustration of how candidate tours satisfy ring requirements

Several candidate tours were developed by the Mission Design Team (MDT) in response to the geometric requirements of the various science working groups and disciplines, including

the Rings Working Group (RWG). These candidate tours have three distinct stages of interest to ring science, which are, naturally, stages containing inclined orbits. An example of these stages is illustrated in figure 6, which is for the tour originally named T18-5 - which has been adopted by the PSG except for small tweaks which remain to be worked out.

5.2.1 Early inclined sequence

In order to satisfy the first RWG "must-have" observation (Section 5.1), the tour includes an early inclined sequence with the node of Cassini's orbit chosen nearly perpendicular to the Saturn-Earth line. This geometry produces nearly ansa-to-ansa diametric occultations for RSS and highly diagnostic illumination and observation geometry for the suite of optical remote sensing (ORS) instruments. The sequence captures the rings near their maximum tilt angle, allowing for an unprecedented opportunity to observe all ring features - including the dense B ring.

All candidate tours were optimized to include this sequence, with the RSS team working with the MDT to achieve optimization of the radio occultations. Tour T18-5 is superb from this standpoint, and at the time of this writing has been selected as the baseline mission tour.

5.2.2 Titan 180° transfer sequence

In order to satisfy the diverse set of geometries needed to meet Cassini's broad science goals, the orbital petal of the spacecraft must be maneuvered to different orientations with respect to the Saturn-Sun direction. This is normally described by changes in the apoapsis phase angle. The orientation of the initial set of orbits is set by the arrival geometry of the spacecraft. The MDT identified a rapid means of achieving a rapid change in apoapsis phase angle by a series of orbits called a Titan 180° transfer (see chapter by Wolf, this volume). These sequences can be divided into two stages: an "up-leg" stage where Cassini flies by Titan at the spacecraft's ascending node (increasing Cassini's orbital inclination and raising its periapse), and a "down-leg" stage where the flyby is at the descending node (decreasing the inclination while lowering the periapse again). These orbits provide high inclinations and also relatively high periapse altitudes.

Critical ORS opportunities to distinguish time and angle varation of fine scale structure occur during the up-leg (to be used in combination with the late, high- inclination sequence, see below). The up-leg stage provides sufficient time for an initial characterization of fine scale ring structure that is known to be either azimuthally or temporally variable (or both), satisfying another "must have" science goal for rings. This structure, often in opaque ring regions, must be observed with high resolution, in backscatter, and on the lit face of the rings. These observations will need to be compared with those that are provided in the final high inclination tour sequence, and so perform a critical time- baseline function. Figure 6 shows that tour T18-5 includes some repeated revs in its single Titan 180° transfer sequence at this critical geometry.

Important RSS opportunities to characterize optical depth dependence and forward ring scatter on the ring opening angle, and hence determine vertical ring structure, occur during the down-leg (when the tilt of the rings as seen from earth is at an intermediate value of

about 15○). The timing of this sequence and the number of repeated revs have important implications for both of these objectives. For this class of orbits, there may be a tradeoff between optimal occultation track geometry and optimal Doppler contour alignment.

5.2.3 Final high inclination sequence

Candidate tours end with the spacecraft in a highly inclined orbit with a low periapse. This geometry is critical to producing the numerous stellar occultation opportunities which are needed for the finest scale studies of ring structure (and particle size). This geometry translates into being close to the planet at high sub-spacecraft latitude, so that the rings present a large target for stellar occultations, and the opaque regions unstudied by Voyager can be probed with good sensitivity. Also, in this geometry ORS captures the other critical part of its observing time in which to study fine scale structure in opaque rings, and azimuthal variations requiring high resolution (requirements 2 and 5, section 5.1). In addition, CIRS requires this geometry to map thermal changes over a ring particle orbit, and RSS requires the low ring tilts provided by this tour stage to observe tenuous ring features (C ring and Cassini Division) and out-of-plane ring features (such as bending waves).

The critical features of this sequence are the high inclination and low periapse altitude. Because this geometry satisfies several "must have" rings requirements (2, 3, and 5), the total number of hours in this "close-in, high-up" geometry must be great enough that the different goals can be met. Because of the low periapse, the amount of time in this geometry on each rev is relatively small, and competition for observing time in this highly favorable geometry for ring observations requires as many revs at as high an inclination as possible. In tour T18-5, this sequence also includes new multiple RSS ring occultation opportunities, though this is not in general a feature of this sequence, and depends on the precise orientation of the orbital petals.

6 Special opportunities

6.1 Saturn Orbit Insertion (SOI)

The brief period immediately following the main engine burn at initial closest approach has been of prime interest for ring science since the pre-Cassini days of the Joint Working Group. During this period, the spacecraft skims the unilluminated side of the rings, with vertical elevation of 10000-30000 km. This is nearly an order of magnitude closer than at any other time during the mission. Even though the smear rate is a few mr/second during this time, the ORS instruments are all sufficiently sensitive that unique new observations can be made with sufficiently short exposure times that smear is not a limitation. The importance of this observing geometry to ring science is easily stated: there are known radial and azimuthal variations in ring structure and composition that will only be resolvable at this time by ORS instruments. CIRS will map the radial variation in ring particle composition at the resolutions of 40-100 km for the far infrared and 3-8 km for the middle infrared. VIMS will resolve radial structure on the several tens of km scale where distinct color and albedo variations are known to exist throughout the rings. ISS, with 6 microradian pixels, should

be able to resolve the 100 m-scale transient density wakes believed to be responsible for the A ring azimuthal brightness asymmetry.

Several studies by the Rings Working Group have shown that a scan of the entire main ring system can be obtained within time constraints, and that ample data volume and signal to noise are available to provide a truly unique data set spanning the extreme UV to the far IR for comparison with all other Cassini data.

6.2 Jupiter encounter

The opportunity to study Jupiter with new instruments (more sensitive than or not carried by Galileo) and excellent spatial resolution (better than HST) allows Cassini to contribute to solving some important and still unresolved problems regarding the faint Jovian ring system, returning more than 10 times the number of ring images obtained by Galileo over a wider range phase and elevation angle than previously. ISS color coverage is greatly expanded over that of Voyager or Galileo, and also has polarization measurement capability (diagnostic of tiny grains). ISS and VIMS will be able to characterize the color and angular scattering behavior of the rings far better than previously. The sparse Galileo images indicate the ring has an azimuthally and/or temporally varying structure, which is too poorly characterized to understand; are these "spokes" in Jupiter's ring? ISS will take "movies" to resolve this question. ISS might also be able to discover new moons in the Jovian vicinity. Although there are some spectral observations of the jovian ring (Nicholson and Matthews 1991, Neugebauer et al. 1981, Smith et al. 1998), the composition of the material comprising the jovian ring remains unknown. Using data collected over several tens of hours in the far infrared, CIRS may be able to ascertain the particle size distribution from the deviation of the spectral emission distribution from a blackbody, or detect silicate absorption features in the mid or far infrared. While Voyager-based photometric analyses support flatter distributions (Showalter et al. 1987), new analyses of the Galileo NIMS data indicate steeper distributions (McMuldroch et al. 2000). It is known that fine dust grains are flying away from Jupiter (Grün et al. 1993, 1996). If the source of any of the dust sampled by CDA can be uniquely identified as the ring or ringmoons, the ring composition might be measured directly. Also, CDA might be able to distinguish between the ring and Io as the ultimate source of ejected fine grains discovered by Galileo (Hamilton and Burns 1993b, Horanyi et al. 1993).

7 Acknowledgements:

Cassini has so far benefitted from the talents and hard work of too many individuals to cite here. Beyond the obvious critical contributions of the highly successful spacecraft, launch, and operations teams, we acknowledge the outstanding work of the Cassini Mission Design Team in helping us through so many varied and complex tours. We also thank Luke Dones for key contributions early in the tour assessment process, and Joe Burns, Ed Danielson, and Mark Showalter for discussions concerning Jupiter's ring system prior to publication. We also acknowledge the valuable support of Kevin Beurle, Ken Bollinger, Jim Bradley, Kevin Grazier, and Brad Wallis in helping us understand the properties of the tour candidates, and Joe Burns and Luke Dones for very thorough reviews of the manuscript.

8 Figure captions

Figure 1: Global view of Saturn's ring system from Voyager 1.

Figure 2: Characteristic structures in Saturn's rings: (a) spiral density and bending waves, typical of the A ring, (b) "irregular structure", typical of the B ring, (c) gap-and-ringlet structure, typical of the C ring and Cassini Division (from Lissauer and Cuzzi 1985).

Figure 3: Typical "spokes", appearing relatively dark at low phase angles (bottom panel) and relatively bright at high phase angles (top panel) due to the scattering properties of the half-micron radius spoke particles relative to the surrounding macroscopic particles. From Cuzzi et al. 1984.

Figure 4: Ring color variations with radial location. Top panel: Overall ring optical depth from stellar occultation data, showing main ring regions: C ring (74510-92000 km), B ring (92000-117580 km), Cassini Division (117580-122170 km), and A ring (122170-136780 km). Middle panel: ring reflectivity or I/F in the Voyager green filter (revised from EC96 to reflect Johnson-Buratti calibration) ; Bottom panel: ratio of reflectivity in Voyager Green filter to that in Voyager UV filter (Voyager "atmospheric" calibration, revised as described in section 3.2).

Figure 5: Schematic of the ringmoon systems of the four giant planets (from Nicholson and Dones 1991), showing how rings and moons intermingle even across the nominal Roche limit.

Figure 6: The observing profile of the baseline tour (T18-5).

9 References

Arakawa, M. and M. Higa (1996) Measurements of ejection velocities in collisional disruption of ice spheres; Planet. Sp. Sci. 44, 901-908

Araki, S. (1988) The dynamics of particle disks, II: Effects of spin degrees of freedom; Icarus, 76, 182-198

Araki, S. (1991a) Dynamics of planetary rings; American Scientist 79, 44-59.

Araki, S. (1991b) The dynamics of particle disks. III - Dense and spinning particle disks; Icarus 90, 139-171

Bauer, J., J. J. Lissauer, and M. Simon (1997) Edge-on observations of Saturn's E and G rings in the near-IR; Icarus, 125, 440-445

Borderies, N. (1989) Ring dynamics; Celestial Mechanics, 46, 207-230

Borderies, N. (1992), Looking for changes in the Saturnian system between Voyager and Cassini; in "Chaos, resonance and collective dynamical phenomena in the solar system", S. Ferraz-Mello (ed.), IAU.

Borderies, N. J., P. Goldreich, and S. Tremaine (1985) A granular flow model for dense planetary rings; Icarus 63, 406-420

Borderies, N. J., P. Goldreich, and S. Tremaine (1986) Nonlinear density waves in planetary rings; Icarus 68, 522-533

Bosh, A. and A. S. Rivkin (1996) Observations of Saturn's inner satellites during the May 1995 ring-plane crossing; Science 272, 518-521

Brahic, A. (1984) Planetary Rings; Proceedings of IAU Colloquium 75; Cepadues-Editions, Toulouse.

Bridges, F. G., K. D. Supulver, D. N. C. Lin, R. Knight, and M. Zafra (1996) Energy loss and sticking mechanisms in particle aggregation in planetesimal formation; Icarus, 123, 422-435

Burns, J. A. (1999) Planetary Rings; in "The New Solar System"; J. Kelly Beatty, ed., Sky Publishing Co.; Third edition.

Burns, J. A. (1986) Some background about satellites; in "Satellites", J. A. Burns and M. S. Matthews, eds, Univ. of Arizona Press

Burns, J. A. and B. Gladman (1998) Dynamically depleted zones for Cassini's safe passage beyond Saturn's rings; Planet. Sp. Sci. 46, 1401-1407

Burns, J.A., D.P. Hamilton, M.R. Showalter, P.D. Nicholson, I. dePater, M. Ockert-Bell, and P. C. Thomas (1999) The formation of Jupiter's faint rings. Science, 284, 1146-1150

Burns, J. A., L. E. Schaffer, R. J. Greenberg, and M. R. Showalter (1985) Lorentz resonances and the structure of Jupiter's rings. Nature 316, 115-119.

Burns, J. A., M. R. Showalter, J. N. Cuzzi, and J. B. Pollack (1980), "Physical processes in Jupiter's ring - Clues to its origin by Jove", Icarus, 44, pp. 339-360

Burns, J. A., M. R. Showalter, and G. A. Morfill (1984) The ethereal rings of Jupiter and Saturn; in "Planetary Rings", R. Greenberg and A. Brahic eds, Univ. of Arizona Press

Canup, R. M. and Esposito, L.W. (1995) Accretion in the roche zone: coexistence of rings and ringmoons; Icarus 113, 331-352

Canup, R. and L. W. Esposito (1997) Evolution of the G ring and the population of macroscopic ring particles; Icarus 126, 28-41

Chakrabarti, S. K. (1989) The dynamics of particles in the bending waves of planetary rings; M. N. R. A. S. 238, 1381-1394

Clark, R. (1980) Ganymede, Europa, Callisto, and Saturn's rings: compositional analysis from reflectance spectroscopy; Icarus 44, 388-409

Clark, R., F. P. Fanale, and M. J. Gaffey (1986) Surface composition of natural satellites; in "Planetary Satellites", J. A. Burns and M. S. Matthews, eds., Univ. of Arizona Press.

Colwell, J. E. (1994) The disruption of planetary satellites and the creation of planetary rings; Planet. Sp. Sci. 42, 1139-1149

Colwell, J. E. and L. W. Esposito (1992) Origins of the rings of Uranus and Neptune. I - Statistics of satellite disruptions; J. Geophys. Res. 97, 10227

Colwell, J. E. and L. W. Esposito (1993), Origins of the rings of Uranus and Neptune. II - Initial conditions and ringmoon populations; J. Geophys. Res. 98, 7387-7401

Colombo, G., P. Goldreich, and A. W. Harris (1976) Spiral structure as an explanation for the asymmetric brightness of Saturn's A ring; Nature, 264, 344

Connerney, J. E. P. (1986) Saturn - A unique magnetosphere/ionosphere/ring interaction; in Comparative study of magnetospheric systems; International Colloquium, Londe-les-Maures, France, September 9-13, 1985, Proceedings Cepadues-Editions, Toulouse; 245-251.

Connerney, J. E. P., and H. Waite (1984) New model of Saturn's ionosphere with an influx of water from the rings; Nature, 312, 136-138

Cooke, M. (1991) Saturn's rings: Photometric studies of the C ring and radial variation in the Keeler gap; unpublished PhD thesis, Cornell University, 1991

Cuzzi, J., (1983) Planetary ring systems, Rev. Geophys. Space Phys. 21, 173-186

Cuzzi, J. N. (1995) Evolution of planetary ring-moon systems; in "Comparative Planetology", Kluwer Press; also, Earth, Moon, and Planets 67; 179-208

Cuzzi, J. N. and J. A. Burns (1988) Charged particle depletion surrounding Saturn's F ring: evidence for a moonlet belt; Icarus, 74, 284-324

Cuzzi, J. N., and R. H. Durisen (1990) Meteoroid bombardment of planetary rings; General formulation and effects of Oort cloud projectiles; Icarus, 84, 467-501

Cuzzi, J. N. and P. R. Estrada (1998) Compositional Evolution of Saturn's Rings due to Meteoroid Bombardment; Icarus, 132, 1-35

Cuzzi, J. N., R. C. French, and L. Dones (2000) HST multicolor photometry (255-1042nm) of Saturn's main rings. I: radial profiles, phase and tilt angle variations, and regional spectra. Icarus, submitted

Cuzzi, J. N., J. J. Lissauer, L. W. Esposito, J. B. Holberg, E. A. Marouf, G. L. Tyler, and A. Boischot (1984) Saturn's Rings: properties and Processes; in "Planetary Rings"; R. Greenberg and A. Brahic, eds. University of Arizona Press

Cuzzi, J. N., J. B. Pollack, and A. L. Summers (1980) Saturn's rings - Particle composition and size distribution as constrained by observations at microwave wavelengths. II - Radio interferometric observations; Icarus, 44, 683-705.] Cuzzi, J. N., and J. D. Scargle (1985) Wavy Edges Suggest Moonlet in Encke's Gap, Astrophys. J. 292, 276-290

Davis, D., S. J. Weidenschilling, C. R. Chapman, and R. Greenberg (1984) Saturn ring particles as dynamic ephemeral bodies; Science 224, 744-747.

de Pater, I., M. R. Showalter, J. A. Burns, P. D. Nicholson, M. C. Liu, D. P. Hamilton, and J. R. Graham (1999) Keck infrared observations of Jupiter's ring system near Earth's 1997 ring plane crossing. Icarus, 138, 214-233

de Pater, I., M. R. Showalter, J. J. Lissauer, and J. R. Graham (1996) Keck infrared observations of Saturn's E and G rings during Earth's 1995 ring plane crossing; Icarus, 121, 195-198

de Pater, I. and J. R. Dickel (1991) Multifrequency radio observations of Saturn at ring inclination angles between 5 and 26 degrees; Icarus 94, 474-492

Divine, N. (1993) Five populations of interplanetary meteoroids; J. Geophys. Res. 98, 17029-17048

Dollfus, A. (1996) Saturn's rings: optical reflectance polarimetry; Icarus 124, 237-261

Dones, L., M. R. Showalter, and J. N. Cuzzi (1989) Simulations of light scattering in planetary rings; in "Dynamics of Astrophysical Disks"; J. Sellwood, ed., Cambridge Univ. Press

Dones, L., J. N. Cuzzi, and M. R. Showalter (1993) Voyager Photometry of Saturn's A ring; Icarus, 105, 184 - 215

Dones, L. (1991) A recent cometary origin for Saturn's rings? Icarus, 92, 194-203

Dones, L. (1997) Saturn's rings, in "Encyclopedia of Planetary Sciences", ed. J.H. Shirley and R.W. Fairbridge, Chapman and Hall

Dones, L. (1998) The rings of the giant planets. In "Solar System Ices"; B. Schmitt, C. de Bergh, and M. Festou, Eds; Kluwer, Dordrecht. 711-734.

Doyle, L. R., L. Dones, and J. N. Cuzzi (1989) Radiative transfer modeling of Saturn's outer B ring; Icarus, 80, 104-135

Doyle, L.R. and E. Grün (1990) Radiative transfer modeling constraints on the size of the spoke particles in Saturn's rings; Icarus 85, 168-190.

Dumas, C., R. J. Terrile, B. A. Smith, G. Schneider, and E. E. Becklin (1999) Stability of Neptune's ring arcs in question; Nature 400, 733-734

Durisen, R. (1984) Transport effects due to particle erosion mechanisms; in "Planetary Rings", R. Greenberg and A. Brahic, eds; Univ. of Az. Press

Durisen, R. H., N. L. Cramer, B. W. Murphy, J. N. Cuzzi, T. L.Mullikin, and S. E. Cederbloom (1989) Ballistic Transport in Planetary Ring Systems due to particle erosion mechanisms. I: Theory, Numerical methods, and illustrative examples; Icarus 80, 136-166

Durisen, R. H., P. W. Bode, J. N. Cuzzi, S. E. Cederbloom, and B. W. Murphy (1992) Ballistic transport in planetary ring systems due to particle erosion mechanisms; II: Theoretical models for Saturn's A- and B- ring inner edges; Icarus, 100, 364 - 393

Durisen, R. H., P. W. Bode, S. G. Dyck, J. N. Cuzzi, J. D. Dull, and J. C. White III (1996) Ballistic transport in planetary ring systems due to particle erosion mechanisms; III: Torques and mass loading by meteoroid impacts; Icarus, 124, 220-236

Elliot, J.L., A. S. Bosh, M. L. Cooke, R. C. Bless, M. J. Nelson, J. W. Percival, M. J. Taylor, J. F. Dolan, E. L. Robinson, and G. W. vanCritters (1993) An occultation by Saturn's rings on 1991 October 2-3 observed with HST; Astron. J. 106, 2544-2572

Epstein, E. E., M. A. Janssen, and J. N. Cuzzi (1984) Saturn's rings - 3-mm low-inclination observations and derived properties, Icarus 58, 403-411

Esposito, L. W. (1993) Understanding planetary rings; in Ann. Rev. Earth and Planet. Sci. 21, 487-523.

Esposito, L. W. (1986) Structure and evolution of Saturn's rings; Icarus, 67, 345-357.

Esposito, L. W., A. Brahic, J. A. Burns, and E. A. Marouf (1991) Physics and microphysics of Uranus' rings; in "Uranus", J. Bergstralh, ed., Univ. of Arizona Press.

Esposito, L. W., R. Canup, and J. E. Colwell (1997) History of Neptune's ring arcs, BAAS 29, 1000

Esposito, L. W., J. N. Cuzzi, J. B. Holberg, E. A. Marouf, G. L. Tyler, and C. C. Porco (1984) Saturn's Rings: Structure, dynamics, and particle properties; in "Saturn", T. Gehrels and M. Matthews, eds. University of Arizona Press

Estrada, P. and J. N. Cuzzi (1996) Voyager Observations of the color of Saturn's Rings; Icarus, 122, 251-272; Also - Erratum Icarus, 125, 474 (1997)

Ferrari, C. and A. Brahic (1994) Azimuthal brightness asymmetries in planetary rings; Icarus, 111, 193-210

Ferrari and Brahic (1997) Arcs and clumps in the Encke division of Saturn's rings; Planet. Space Science; 45, 1051-1067

Feuchtgruber, H., E. Lellouch, T. de Graauw, B. Bezard, T. Encrenaz, and M. Griffin (1997) External supply of oxygen to the atmospheres of the giant planets; Nature, 389, 159-162

Flynn, B.C., and J. N. Cuzzi (1989); Regular structure in the Cassini Division of Saturn; Icarus, 82, 180-199

Foryta, D. W. and B. Sicardy (1996) The dynamics of the Neptunian Adams ring's arcs; Icarus 123, 129-167

Fouchet, T., R. Prange, J. E. C. Connerney, R. Courtin, L. Ben Jaffel, K. Noll, and J. C. McConnell (1996) HST spectro-imaging of Saturn and search for water from the rings; 28th DPS, Tucson, poster 19.07

French, R. G., P. D. Nicholson, C. C. Porco, and E. A. Marouf (1991) Dynamics and structure of the Uranian rings; in "Uranus", University of Arizona Press, Tucson, AZ, p. 327-409.

French, R.G., P. D. Nicholson, M. L. Cooke, J. L. Elliot, K. Matthews, O. Perkovic, E. Tollestrup, P. Harvey, N. J. Chanover, M. A. Clark, E. W. Dunham, W. Forrest, J. Harrington, J. Pipher, A. Brahic, I. Grenier, F. Roques, and M. Arndt (1993); Geometry of the Saturn system from the 3 July 1989 occultation of 28 Sgr and Voyager observations; Icarus 103, 163-214.

French, R. C., J. Cuzzi, R. Danos, L. Dones, and J. Lissauer (1998a) Hubble space telescope observations of spokes in Saturn's rings; "The Jovian system after Galileo, the Saturnian system before Cassini-Huygens; Cite' des Congres, Nantes, France; 11-15 May 1998.

French, R. G. D. Graham, J. Cuzzi, L. Dones, and J. Lissauer (1998b) "Hubble Space Telescope observations of Saturn's rings: the opposition effect" BAAS 30, 1045–1046. 30th DPS Meeting, Madison

French, R. G., C. A. McGhee, P. D. Nicholson, L. Dones, and J. Lissauer (1999) Saturn's wayward shepherds: Pandora and Prometheus; B. A. A. S. 31, number 4.

Gehrels, T. and M. S. Matthews (1984) "Saturn"; University of Arizona Press.

Goertz, C. K. and G. Morfill (1983) A model for the formation of spokes in Saturn's rings; Icarus, 53, 219-229.

Goertz, C. (1984) Formation of Saturn's spokes; Advances in Space Research vol. 4, no. 9, 1984, p. 137-141.

Goertz, C.K., G. E. Morfill, W.-H.-Ip, E. Grün, and O. Havnes (1986) Electromagnetic angular momentum transport in Saturn's rings; Nature 320, 141-143.

Goldreich, P. and C. C. Porco (1987) Shepherding of the Uranian Rings. II. Dynamics; Astron. J. 93, 730

Goldreich, P. and S. Tremaine (1982); The dynamics of planetary rings; Ann. Revs. Astron. Astrophys. 20, 249-283

Goldreich, P., S. Tremaine, and N. Borderies (1986) Towards a theory for Neptune's arc rings; Astron. J. 92, 490-494

Gordon, M., C. D. Murray, and Beurle (1996) Further evidence for the existence of additional small satellites of Saturn; Icarus, 121, 114-125

Greenberg, R. and A. Brahic (1984) Planetary Rings, University of Arizona Press

Gresh, D., P. A. Rosen, and G. L. Tyler (1986) An analysis of bending waves in Saturn's rings using Voyager radio occultation data; Icarus 68, 481-502

Grossman, A. (1991) Microwave imaging of Saturn's deep atmosphere and rings; unpublished PhD thesis, California Institute of Technology

Grossman, A. W., D. O. Muhleman, and G. L. Berge (1989) High-resolution microwave images of Saturn; Science, 245, 1211-1215

Grün, E., G. E. Morfill, and A. Mendis (1984a) Dust-magnetosphere interactions; in "Planetary Rings", R. Greenberg and A. Brahic, eds; U. of Az. Press

Grün, E., R. J. Garneau, R. J. Terrile, T. V. Johnson, and G. E. Morfill (1984b) Kinematics of Saturn's spokes; Adv. Sp. Res. 4, 143-148.

Grün, E., C. K. Goertz, G. E. Morfill, and O. Havnes (1992) Statistics of Saturn's spokes; Icarus vol. 99, 191-201.

Grün, E., P. Staubach, M. Baguhl, D. P. Hamilton, H. A. Zook, S. Dermott, B. A. Gustafson, H. Fechtig, J. Kissel, D. Linkert, G. Linkert, R. Srama, M. S. Hanner, C. Polanskey, M. Horanyi, B. A. Lindblad, I. Mann, Ja. M. McDonnell, G. E. Morfill, and G. Schwehm (1997) South-North and radial traverses through the interplanetary dust cloud; Icarus, 129, 270-288.

Grün, E., and 21 co-authors (1996) Constraints from Galileo observation on the origin of Jovian dust streams. Nature 381, 395-98.

Grün, E., and 22 co-authors (1993) Discovery of jovian dust streams and interstellar grains by the Ulysses spacecraft. Nature 362, 428-30

Hall, D. T., P. D. Feldman, J. B. Holberg, and M. A. McGrath (1996) Fluorescent hydroxyl emissions from Saturn's ring atmosphere; Science, 272, 516-518

Hamilton, D. P., and J. A. Burns (1993) OH from Saturn's rings. Nature 365, 498.

Hamilton, D. P. and J. A. Burns (1993) The ejection of dust from Jupiter's gossamer ring. Nature 364, 695-699

Hamilton, D. P., and J. A. Burns (1994) Origin of Saturn's E ring: Self-sustained, naturally. Science 264, 550-553.

Hänninen, J. (1993) Numerical simulations of moon-ringlet interaction; Icarus 103, 104-123

Hänninen, J. and H. Salo (1992) Collisional simulations of satellite Lindblad resonances; Icarus 97, 228-247

Hänninen, J. and H. Salo (1994) Collisional simulations of satellite Lindblad resonances; II: Formation of narrow ringlets; Icarus 108, 325-346

Hänninen, J. and H. Salo (1995) Formation of isolated narrow ringlets by a single satellite; Icarus 117, 435-438

Hänninen, J. and C. C. Porco (1997) Collisonal simulations of Neptune's ring arcs; Icarus 126, 1-27

Hapke, B. (1990) Coherent backscatter and the radar characteristics of the outer planet satellites; Icarus 88, 407-417

Hapke, B. and D. Blewett (1991) Coherent backscatter model for the unusual radar refelctivity of icy satellites; Nature 352, 46-47

Harrington, J., M. L. Cooke, W. J. Forrest, J. L. Pipher, E. W. Dunham, and J. L. Elliot (1993) IRTF observations of the occultation of 28 Sgr by Saturn; Icarus 103, 235-252.

Harris, A. W. (1984) The origin and evolution of planetary rings; in "Planetary Rings", R. Greenberg and A. Brahic, eds; U. of Az. Press

Helfenstein, P., N. Currier, B. E. Clark, J. Veverka, M. Bell, R. Sullivan, J. Klemaszewski, R. Greeley, R. T. Pappalardo, J. W. Head III, T. Jones, K. Klaasen, K. MaGee, P. Geissler, R. Greenberg, A. McEwen, C. Phillips, T. Colvin, M. Davies, T. Denk, G. Neukum, and M. J. S. Belton (1998) Galileo observations of Europa's opposition effect; Icarus 135, 41-63

Higa, M. M. Arakawa, and N. Maeno (1996) Measurements of restitution coefficients of ice at low temperature; Planet. Space Sci. 44, 917-925

Horanyi, M., J.A. Burns, and D. P. Hamilton (1992) The dynamics of Saturn's E ring particles. Icarus 97, 248-259.

Horanyi, M., and T.E. Cravens (1996) The structure and dynamics of Jupiter's ring. Nature 381, 293-295.

Horanyi, M., G. E. Morfill and E. Grün (1993) Mechanism for the acceleration and ejection of dust grains from Jupiter's magnetosphere. Nature 363 144-146

Horn, L.J. (1997) Planetary rings, in "Encyclopedia of Planetary Sciences", ed. J.H. Shirley and R.W. Fairbridge, Chapman and Hall, 602-607

Horn, L. J., and J. N. Cuzzi, (1996) Characteristic wavelengths of irregular structure in Saturn's B and A rings; Icarus, 119, 285-310

Horn, L. J., M. R. Showalter, and C. T. Russell, (1996) Detection and behavior of Pan wakes in Saturn's A ring; Icarus, 124, 663-676

Hubbard, W.B., C. C. Porco, D. M. Hunten, G. H. Rieke, M. J. Rieke, D. W. McCarthy, V. Haemmerle, R. Clark, E. P. Turtle, J. Haller, B. McLeod, L. A. Lebofsky, R. Marcialis, J. B. Holberg, R. Landau, L. Carrasco, J. Elias, M. W. Buie, S. E. Persson, T. Boroson, S. West, and D. J. Mink (1993) The occultation of 28 Sgr by Saturn - Saturn pole position and astrometry; Icarus 103, 215-234.

Ip, W-H (1983) Collisional interactions of ring particles; ballistic transport process; Icarus 54, 253-262

Ip, W-H (1984) Ring torque of Saturn from interplanetary meteoroid impact; Icarus 60, 547-552

Ip, W-H. (1995a) The exospheric systems of Saturn's rings; Icarus, 115, 295-303

Ip, W-H. (1995b) Implications of meteoroid-ring interactions for observations of the 1995 Saturn ring plane crossing; Icarus 117, 212-215

Karkoschka, E. (1994) Spectrophotometry of the jovian planets and Titan at 300-1000 nm wavelength; The methane spectrum; Icarus 111, 174-192

Karkoschka, E. (1997) Rings and satellites of Uranus: Colorful and not so dark; Icarus 125, 348-363

Kolvoord, R., J. A. Burns, and M. R. Showalter (1990) Periodic features in Saturn's F ring - Evidence for nearby moonlets; Nature 345, 695-697.

Lin, D. N. C and P. Bodenheimer (1981) On the stability of Saturn's rings; Astrophys. J. 248, L83 - L86

Lissauer, J. J. (1984) Ballistic transport in Saturn's rings; An analytic theory; Icarus 57, 63-71

Lissauer, J. J. (1985) Shepherding model for Neptune's arc ring; Nature, 318, 544-545

Lissauer, J. J., P. Goldreich, and S. Tremaine (1985) Evolution of the Janus-Epimetheus coorbital resonance due to torques from Saturn's rings; Icarus 64, 425-434

Lissauer, J. J., F. H. Shu, and J. N. Cuzzi (1981) Moonlets in Saturn's rings? Nature 292, 707-711

Lissauer, J.J. and S.J. Peale (1986) The production of 'braids' in Saturn's F ring; Icarus, 67, 358-374

Lissauer, J. J., S. W. Squyres, and W. K. Hartmann (1988) Bombardment history of the Saturn system; J. Geophys. res 93, 13776-13804

Lissauer, J. J., and J. N. Cuzzi (1985) Rings and moons - Clues to understanding the solar nebula; in Protostars and Planets, D. Black and M. S. Matthews, eds, Univ. of Arizona Press

Longaretti, P.-Y. (1989) Saturn's main ring particle size distribution: An analytic approach; Icarus 81, 51-73

Longaretti, P.-Y. and N. Rappaport (1995) Viscous overstabilities in dense narrow planetary rings; Icarus 116, 376-396

Marley, M. S., and C. C. Porco (1993) Planetary acoustic mode seismology: Saturn's rings; Icarus 106, 508-524

Marouf, E. A., G. L. Tyler, H. A. Zebker, R. A. Simpson, and V. R. Eshleman (1983). Particle size distributions in Saturn's rings from Voyager 1 radio occultation. Icarus 54, 189-211

Marouf, E. A. and G. L. Tyler (1986). Detection of two satellites in the Cassini Division of Saturn's rings. Nature 323, 31-35

Marouf, E. A., G. L. Tyler, and P. A. Rosen (1986). Profiling Saturn's rings by radio occultation. Icarus, 68, 120-166

McMuldroch, S., G. E. Danielson, S. H. Pilorz, and the NIMS science team (2000) Galileo NIMS near-infrared observations of Jupiter's ring system; Icarus, submitted.

Meyer-Vernet, N., A. Lecacheux, and B. M. Pedersen (1998) Constraints on Saturn's G ring from the Voyager 2 radio astronomy experiment; Icarus 132, 311-320

Mishchenko, M. I. and J. M. Dlugach (1992) Can weak localization of photons explain the opposition effect of Saturn's rings? Mon. Not. Roy. Ast. Soc., 254, 15p-18p

Molnar, L. A. and D. E. Dunn (1995) The Mimas 2:1 eccentric corotational resonance in Saturn's outer B ring; Icarus, 116, 397-408

Molnar, L. A., D. E. Dunn, and J. D. Fix (1998) VLA observations of Saturn's rings; Icarus, submitted

Morfill, G. E., H. Fechtig, E. Grün, and C. K. Goertz (1983) Some consequences of meteoroid impacts on Saturn's rings; Icarus 55, 439-447

Moses, J. (1998) Micrometeoritic bombardment of Saturn. I. Ablation profiles; LPSC Abstracts 1998

Moses, J., B. Bezard, E. Lellouch, H. Feuchtgruber, and M. Allen (1998) Micrometeoritic bombardment of Saturn. II. Implied total flux and effects on photochemistry; LPSC Abstracts 1998

Mosqueira, I. (1996) Local simulations of perturbed dense planetary rings; Icarus 122, 128-152

Mosqueira, I., P. R. Estrada, and L. Brookshaw (1999) Hydrodynamical simulations of narrow planetary rings; I: Scaling; Icarus, 139, 260-285.

Murray, C. D. and S. M. Giuliatti-Winter (1996) Periodic collisions between the moon Prometheus and Saturn's F ring; Nature, 380, p. 139-141

Murray, C. D., M. K. Gordon, and S. M. Giuliatti-Winter (1997) Unraveling the strands of Saturn's F ring; Icarus 129, 304-316

Neugebauer, G., E. Becklin, D. C. Jewitt, R. J. Terrile, and G. E. Danielson (1981) Spectra of the Jovian ring and Amalthea; Astron. J. 86, 607-610

Nicholson, P. D. and L. Dones (1991) Planetary rings; Rev. Geophys. Supp. 29, pt. 1, 313-327.

Nicholson, P. D. and R. G. French (1998) particle sizes in Saturn's rings derived from stellar occultation data; BAAS 30, 1043; Icarus, submitted.

Nicholson, P. D., I. Mosqueira, and K. Matthews (1995) Stellar occultation observations of Neptune's rings: 1984-1988; Icarus, 113, 295-330

Nicholson, P. D., D. P. Hamilton, K. Matthews, and C. F. Yoder (1992) New observations of Saturn's coorbital satellites; Icarus, 100, 464-484

Nicholson, P. D. and K. Matthews (1991) Near-infrared observations of the Jovian ring and small satellites; Icarus, 93, 331-346.

Nicholson, P. D.; Showalter, M. R.; Dones, L.; French, R. G.; Larson, S. M.; J. J. Lissauer, C. A. McGhee, P. Seitzer, B. Sicardy, and G. E. Danielson (1996) Observations of Saturn's ring-plane crossings in August and November 1995; Science 272, 509-515

Northrop, T. G. and J. R. Hill (1982) Stability of negatively charged grains in Saturn's ring plane; J. Geophys. Res. 87, 6045-6051

Northrop, T. G. and J. R. Hill (1983) The adiabatic motion of charged grains on rotating magnetospheres; J. Geophys. Res. 88, 1-11

Ockert, M. E., J. N. Cuzzi, C. C. Porco, and T. V. Johnson (1987) Photometry of the Uranian rings from Voyager; J. Geophys. Res., 92, 14969-14979

Ockert-Bell, M.E., J.A. Burns, I.J. Daubar, P.C.Thomas, J. Veverka, M.J.S. Belton, and K.P. Klaasen (1999) The structure of Jupiter's ring system as revealed by the Galileo imaging experiment. Icarus 138, 188-213

Osterbart, R. and E. Willerding (1995) Collective processes in planetary rings; Planet. Space. Sci 43, 289-298

Paranicas, C. and A. F. Cheng (1997) A model of satellite microsignatures at Saturn; Icarus 125, 380-396

Porco, C. C. (1990) Narrow rings: Observation and theory. Adv. Space Res. 10, (1), 221-229.

Porco, C. C. (1991) An Explanation for Neptune's Ring Arcs. Science, 253, 995-1001.

Porco, C. C. (1995) Highlights in planetary rings; Revs. Geophys. Sp. Phys. Supp. July 1995, pp. 497-504

Porco, C. and Danielson, G.E. (1982). The Periodic Variation of Spokes in Saturn's Rings, Astron. J. 87, 826.

Porco, C. C. and Danielson, G. E. (1984). The kinematics of spokes. Proceedings of the IAU Colloquium # 75, Planetary Rings, A. Brahic, Ed., CNES, Toulouse, France.

Porco, C. C. and P. Goldreich (1987) Shepherding of the Uranian rings. I - Kinematics. Astron. J. 93, 724-737.

Porco, C. C., P. D. Nicholson, J. J. Lissauer, J. N. Cuzzi, and L. W. Esposito (1995) Neptune's Rings; in "Neptune and Triton; D. Cruikshank, ed.; University of Arizona Press

Poulet, F., E. Karkoschka, and B. Sicardy (1999) Spectrophotometry of Saturn's small satellites and rings from Hubble Space Telescope images; J. Geophys. Res. 104, E10, 24095-24110

Poulet, F. , B. Sicardy, P. Nicholson, E. Karkoschka, and J. Caldwell (1998) Saturn's ring plane crossings of August and November 1995: A model for the new F ring objects; submitted to Icarus

Rappaport, N. (1998) Ring-ringlet interactions; Icarus, 132, 36-42

Ring Hazard Working Group (1991) Abundance and size of ring material outside the main rings of Saturn; in Cassini AO OSSA-1-91 (JPL PD699-11), Volume XIII, Physical Models.

Ring Hazard Working Group (1996) unpublished report of Second Ring Hazard Workshop, Ames Research Center, January 1996.

Richardson, D. (1994) Tree code simulations of planetary rings; Mon. Not. Roy. Ast. Soc, 269, 493

Roddier, C.; F. Roddier, J. E. Graves, O. Guyon, M. J. Northcott, and B. Sicardy (1999) Rings of Neptune; IAU Circ., 7108, 3

Roddier, C., F. Roddier, J. E. Graves, and M. J. Northcott, (1998) Discovery of an Arc of Particles near Enceladus' Orbit: A Possible Key to the Origin of the E Ring; Icarus, 136, 50-59.

Rosen, P. A. and J. J. Lissauer (1988) The Titan 1:0 nodal bending wave in Saturn's rings; Science 241, 690-694

Rosen, P. A., G. L. Tyler, and E. A. Marouf (1991a) Resonance structures in Saturn's rings probed by radio occultation; I: Methods and examples; Icarus 93, 3-24

Rosen, P. A., G. L. Tyler, E. A. Marouf, and J. J. Lissauer (1991b) Resonance structures in Saturn's rings probed by radio occultation; II: Results and interpretation; Icarus 93, 25-44

Salo, H. (1991) Numerical simulations of dense, collisional systems; Icarus 90, 254-270; erratum Icarus 92, 367-368

Salo, H. (1992a) Numerical simulations of dense, collisional systems; II. Extended distribution of particle sizes; Icarus 96, 85-106

Salo, H. (1992b) Gravitational wakes in Saturn's rings; Nature, 359, 619-621

Salo, H. (1995) Simulations of dense planetary rings; Icarus 117, 287-312

Salo, H. and J. Hänninen (1998) Neptune's partial rings: Action of Galatea on self-gravitating arc particles; Science 282, 1102-1104

Scargle, J. D., J. Cuzzi, A. Dobrovolskis, L. Dones, R. Hogan, C. Levit, M. Showalter, and K. Young (1993); Dynamical evolution of Saturn's rings; B.A.A.S. 25, 3, 1103

Schaffer, L.E., and J.A. Burns (1987) The dynamics of weakly charged dust: Motion through Jupiter's gravitational and magnetic fields. JGR 92, 2264-2280.

Schaffer, L., and J.A. Burns (1992) Lorentz resonances and the vertical structure of dusty rings: Analytical and numerical results. Icarus 96, 65-84.

Schmit, U. and W. M. Tscarnuter (1995) A fluid dynamical treatment of the common action of self-gravitation, collisions, and rotation in Saturn's B ring; Icarus 115, 304-319

Showalter, M. R., K. J. Bollinger, J. N. Cuzzi, and P. D. Nicholson (1996) The rings node of the planetary data system; Planet. Space Sci. 44, 33-45

Showalter, M. R., J. A. Burns, J. N. Cuzzi, and J. B. Pollack (1987) Jupiter's ring: New results on structure and particle properties from Voyager photometry; Icarus, 69, 458-498

Showalter, M. R. (1996) Saturn's D ring in the Voyager images; Icarus 124, 677-689

Showalter, M. R., J. B. Pollack, M. E. Ockert, L. Doyle, and J. B. Dalton (1992) A photometric study of Saturn's F ring; Icarus 100, 394-411

Showalter, M. R., J. N. Cuzzi, and S. M. Larson (1991) Groundbased and Voyager photometry of Saturn's E ring; Icarus, 94, 451-473

Showalter, M. R., and J. N. Cuzzi (1993) Seeing ghosts: Photometry of Saturn's G ring; Icarus 103, 124 - 143

Showalter, M. R. and P. D. Nicholson (1990) Saturn's rings through a microscope: Particle size constraints from the Voyager PPS scan; Icarus 87, 285-306

Showalter, M. R., J. N. Cuzzi, E. A. Marouf, and L. W. Esposito (1986), Moonlet wakes and the orbit of the Encke gap moonlet; Icarus, 66, 297-323

Showalter, M. R. (1991) Visual detection of 1981 S13, Saturn's 18th satellite, and its role in the Encke gap; Nature, 351, 709-713

Showalter, M. R. (1998) Detection of impact events in Saturn's F ring; Science, 282, 1099-1102

Shu, F. H., Dones, L., Lissauer, J. J., Yuan, C., Cuzzi, J. N. (1985), "Nonlinear Spiral Density Waves: Viscous Damping", Astrophys. J. 299, 542-573

Sicardy, B., F. Roddier, C. Roddier, E. Perozzi, J. E. Graves, O. Guyon, and M. J. Northcott (1999) Images of Neptune's ring arcs obtained by a ground-based telescope; Nature, 400, 731-732

Smith, B. A., L. A. Soderblom, R. Batson, P. Bridges, J. Inge, H. Masursky, E. M. Shoemaker, R. F. Beebe, J. Boyce, G. A. Briggs, A. Bunker, S. A. Collins, C. J. Hansen, T. V. Johnson, J. L. Mitchell, R. J. Terrile, M. H. Carr, A. F. Cook II, J. N. Cuzzi, J. B. Pollack, G. E. Danielson, A. P. Ingersoll, M. E. Davies, G. E. Hunt, D. Morrison, T. Owen, C. Sagan, J. Veverka, R. G. Strom, and V. E. Suomi (1982). A new look at Saturn: The Voyager 2 images. Science 215, 504-537

Smith, B. A., R. Meier, T. C. Owen, E. Becklin, and and R. J. Terrile (1998) Near-infrared photometry of the Jovian Ring with NICMOS; in preparation; also B.A.A.S. 30, 1040

Supulver, K. D., F. G. Bridges, S. Tiscareno, J. Lievore, D. N. C. Lin (1997) The sticking properties of water frost produced under various ambient conditions; Icarus 129, 539-554

Tagger, M.; Henriksen, R. N.; Pellat, R. (1991) On the nature of the spokes in Saturn's rings; Icarus 91, 297-314.

Terrile, R. J., C. Dumas, B. A. Smith, M. Rieke, G. Schneider, R. Thompson, E. Becklin, and D. Koerner (1998) First infrared imaging of the Neptune ring arcs: HST/NICMOS results; B.A.A.S. 30, 1044.

Throop, H. B. and L. W. Esposito (1998) G ring particle sizes derived from ring plane crossing observations; Icarus 131, 152-166.

Tyler, G. L., E.A. Marouf, R. A. Simpson, H. A. Zebker, and V. R. Eshleman (1983). The microwave opacity of Saturn's Rings at Wavelengths of 3.6 and 13 cm from Voyager 1 Radio Occultation. Icarus 54, 160-188

Van Allen, J. A. (1983) Absorption of energetic particles by Saturn's ring G; J. Geophys. Res. 88, A9, 6911-6918

Van Allen, J. A. (1984) Energetic particles in the inner magnetosphere of Saturn; in "Saturn", T. Gehrels and M. S. Matthews, eds, Univ. of Az. Press

van der Tak, F., I. de Pater, A. Silva, and R. Millan (1998) Time variability in the radio brightness distribution of Saturn; Icarus, submitted.

Ward, W. R. (1981) On the radial structure of Saturn's rings; Geophys. Res. Lett. 8, 641-643

Wisdom, J. and S. Tremaine (1988) Local simulations of planetary rings; Astron. J. 95, 925-940

Yoder, C. F. S. P. Synnott, and G. L. Tyler (1989) Orbits and masses of Saturn's co-orbiting satellites Janus and Epimetheus; Astron. J. 98, 1875-1889

Zebker, H. A., E. A. Marouf, and G. L. Tyler (1985); Saturn's rings; particle size distribution for thin layer models; Icarus 64, 531-548

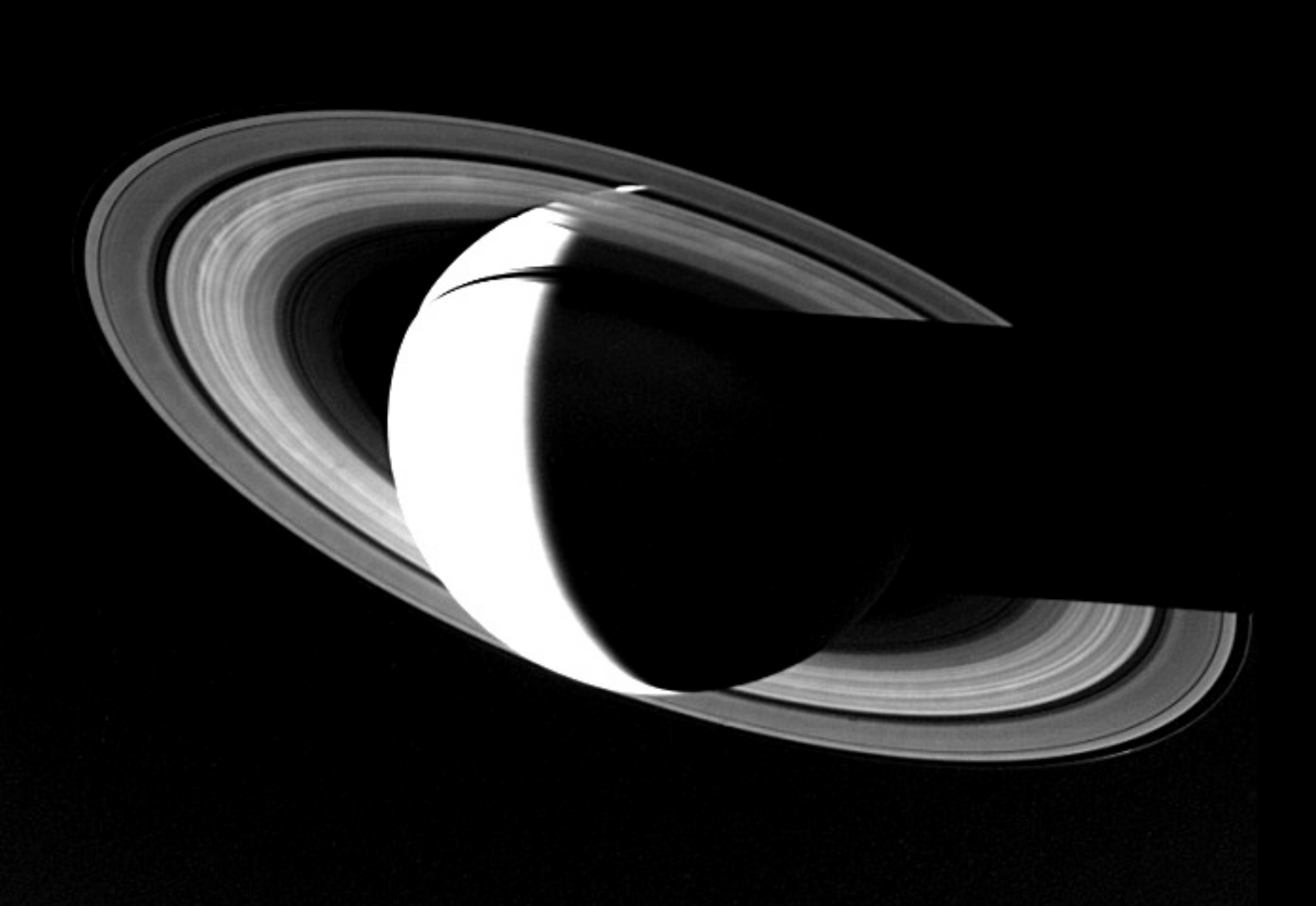

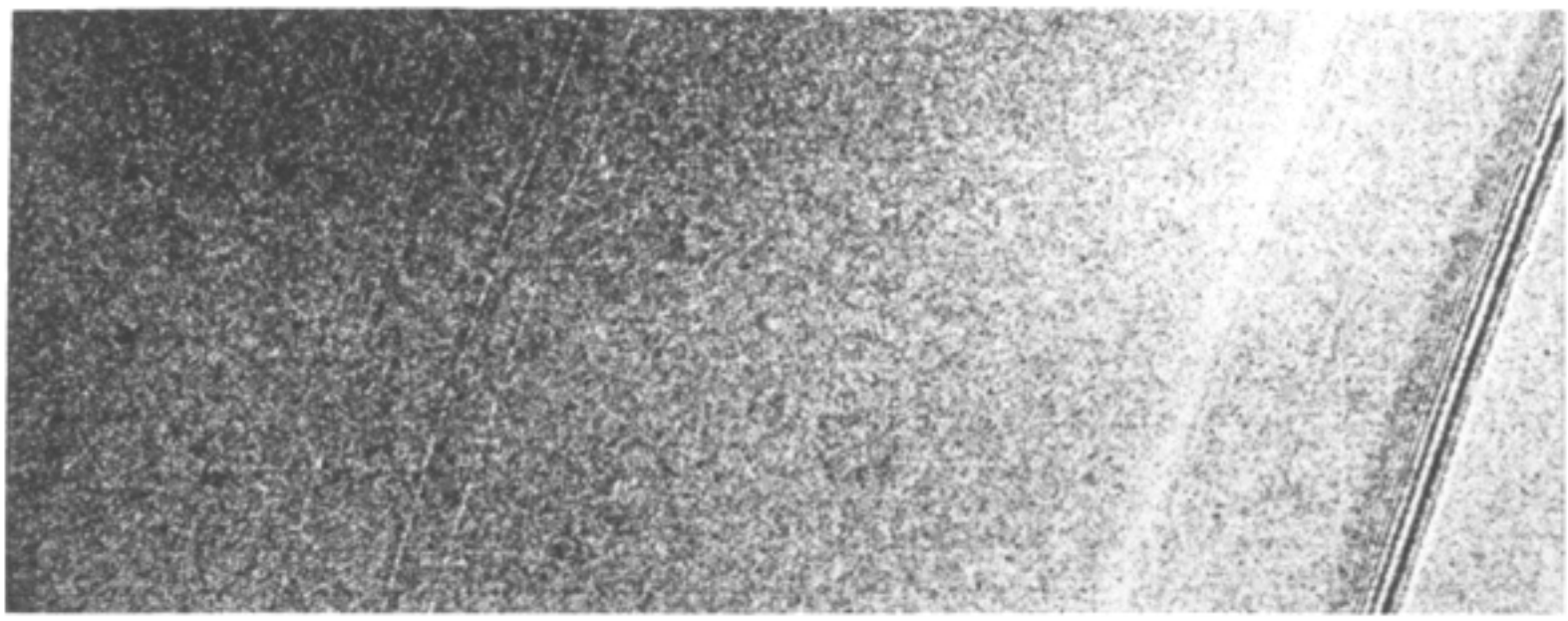

A

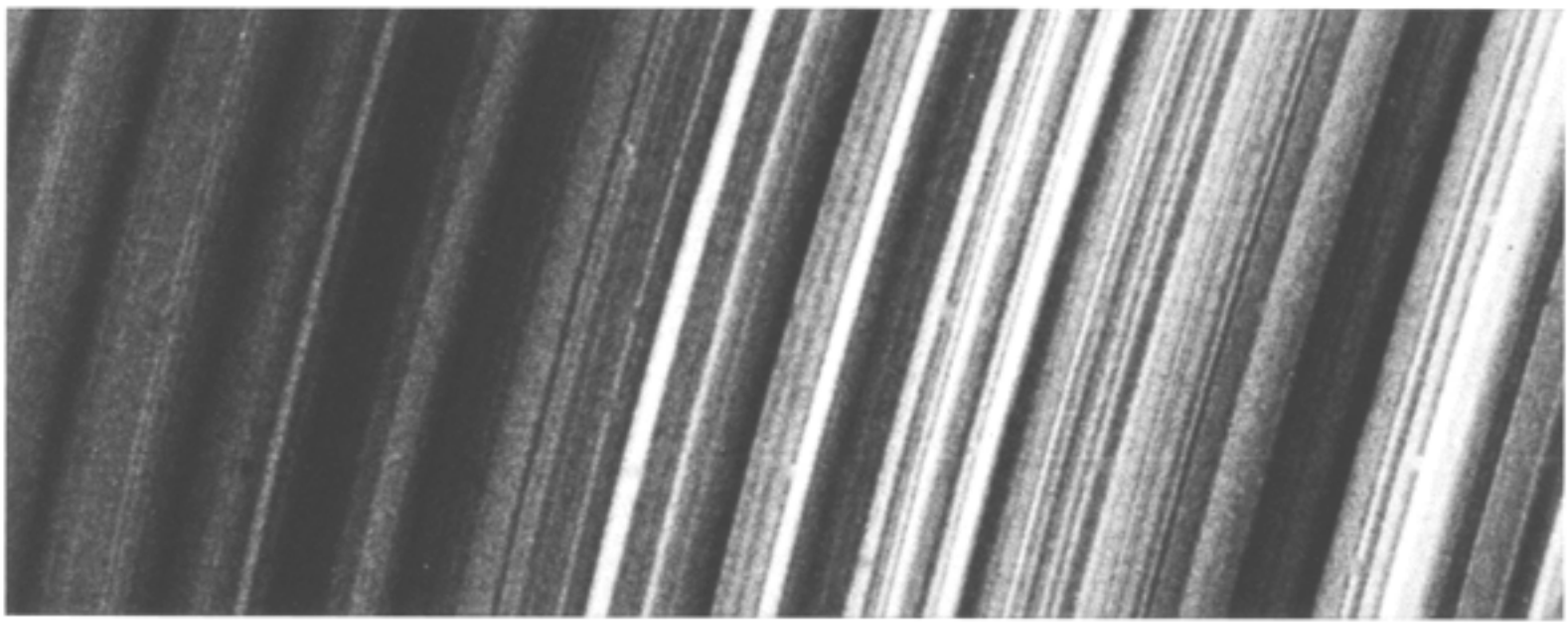

B

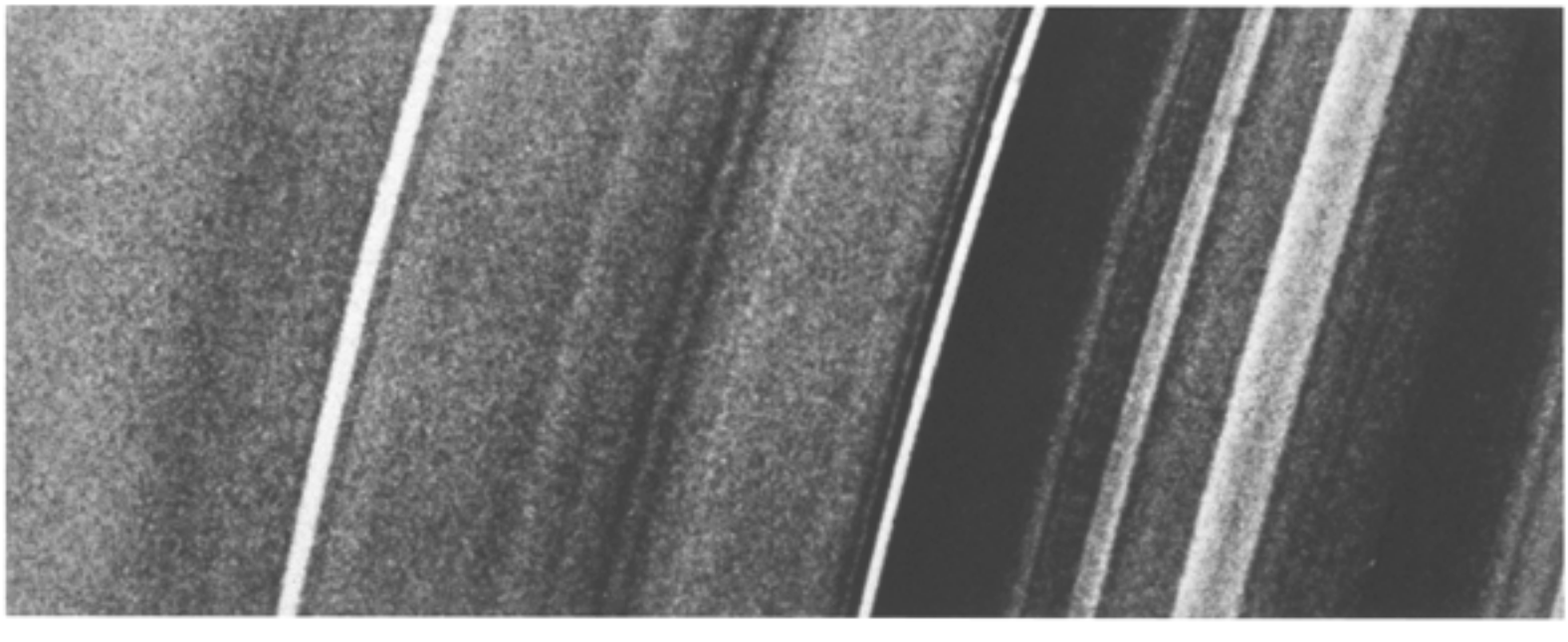

C

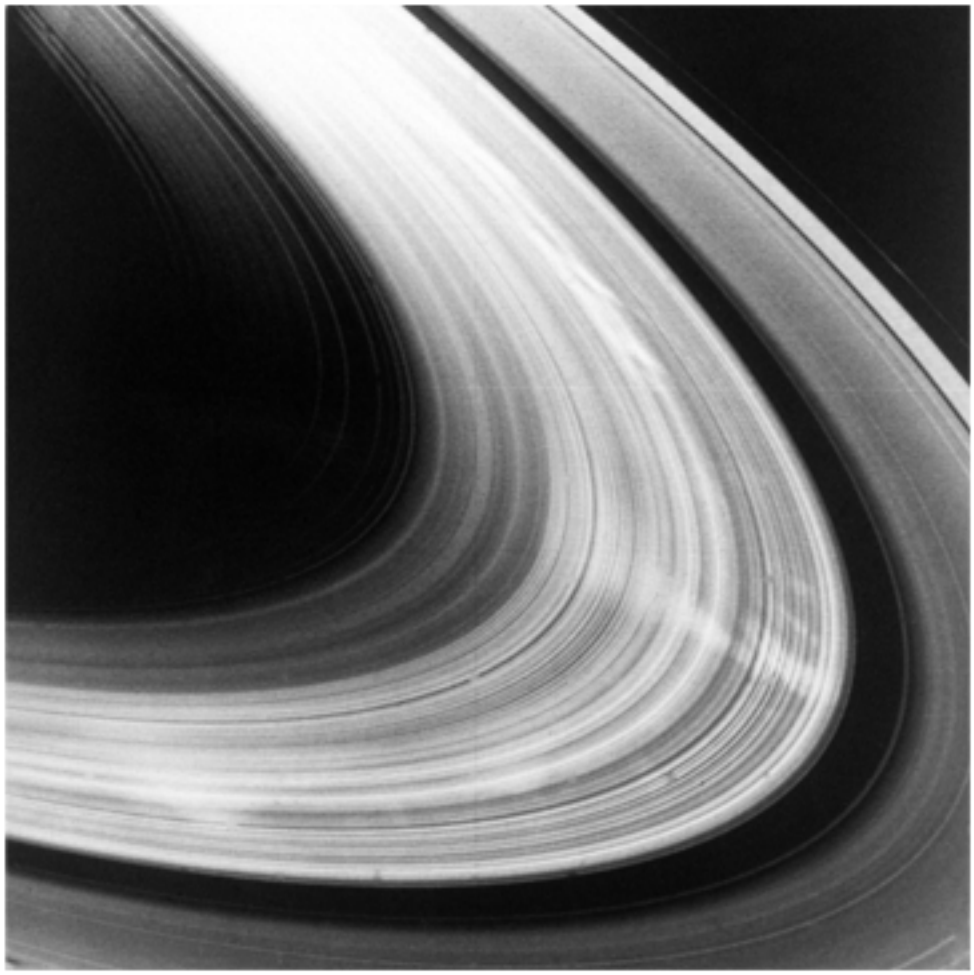

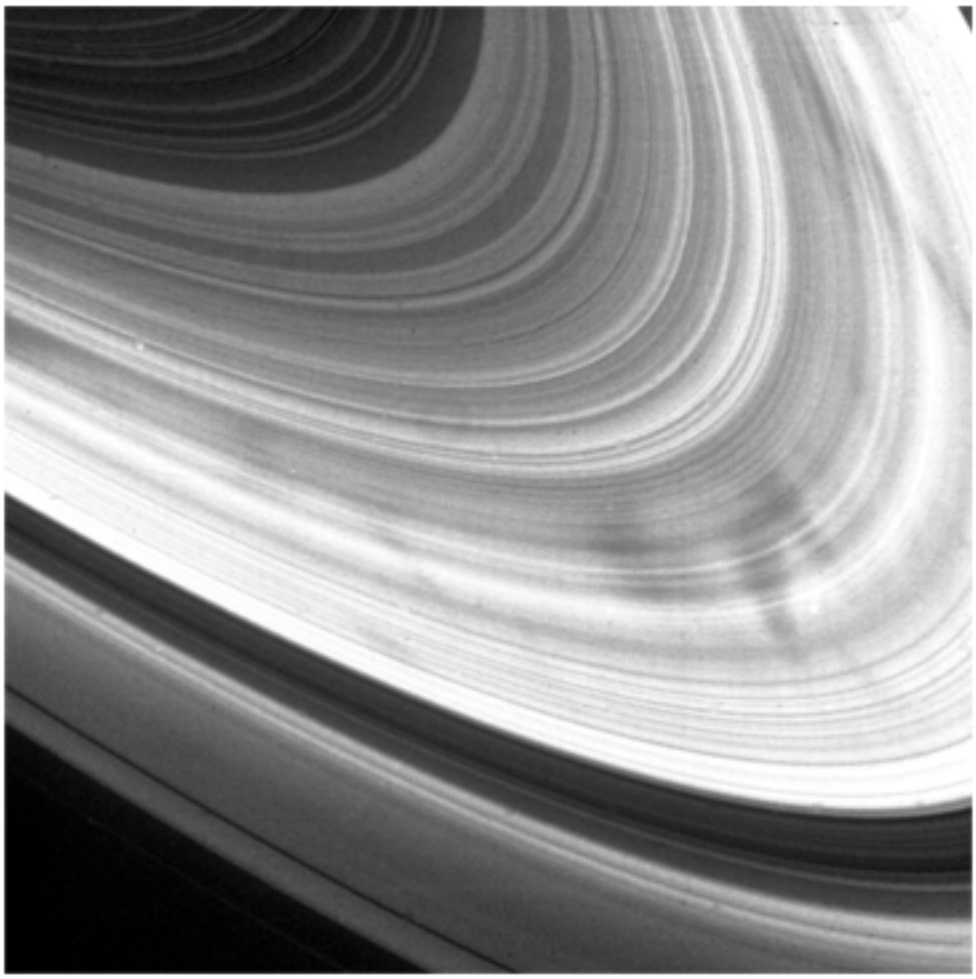

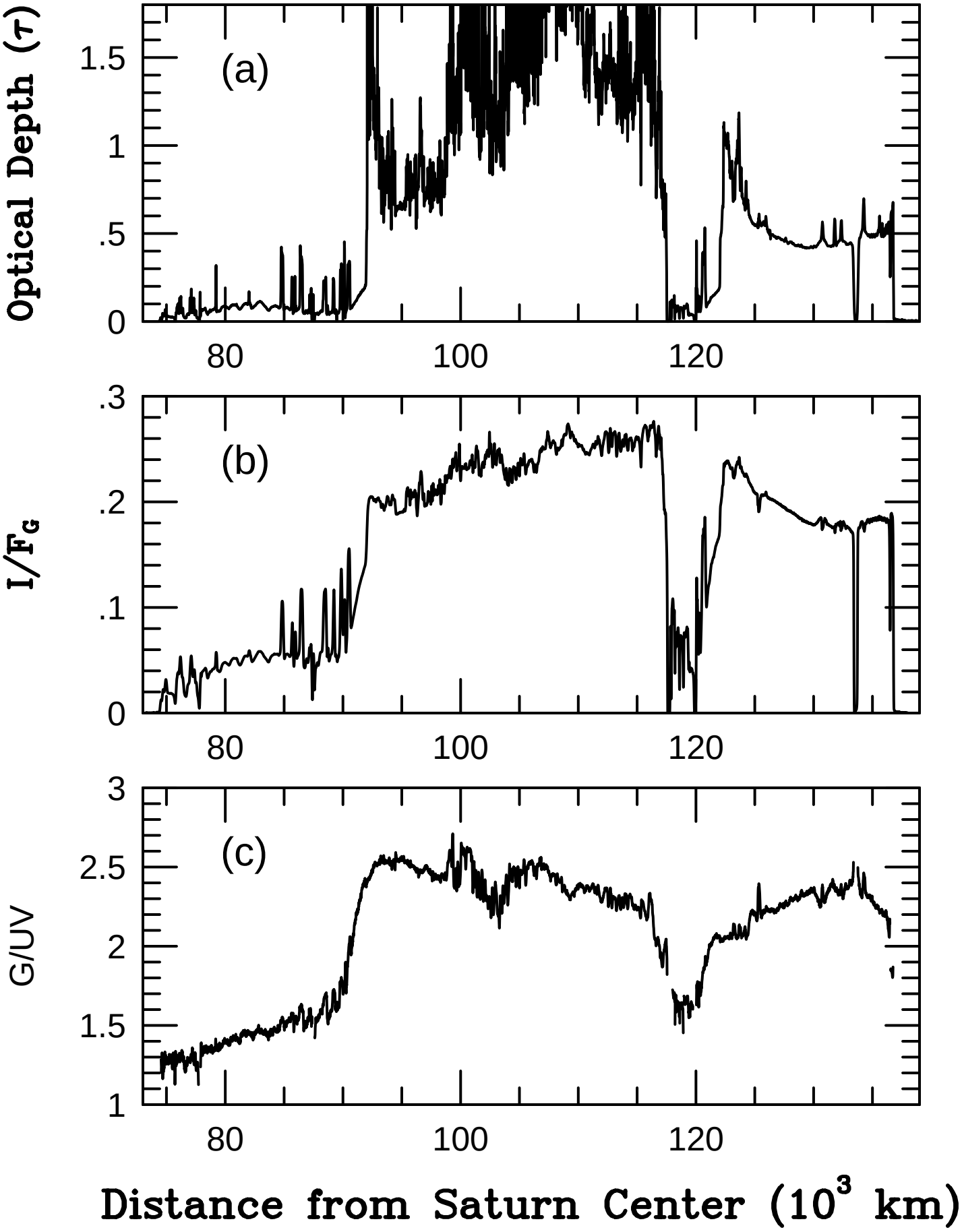
Optical Depth (τ)
(a)
1.5
1
.5
0
80
100
120
I/F_G
(b)
.3
.2
.1
0
80
100
120
G/UV
(c)
3
2.5
2
1.5
1
80
100
120
Distance from Saturn Center (10^3 km)

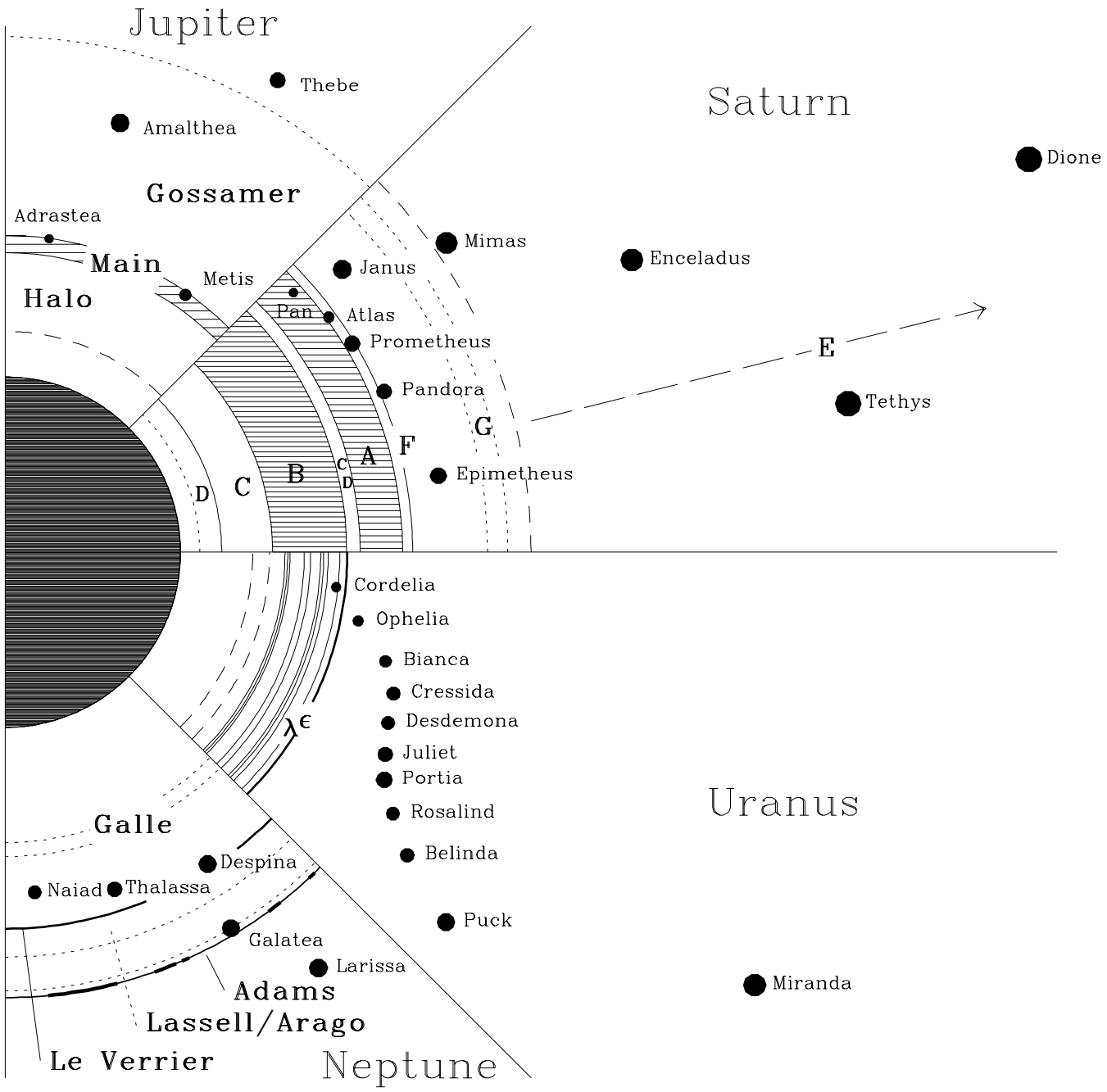
Jupiter
Thebe
Amalthea
Gossamer
Adrastea
Main
Halo
Metis
Saturn
Dione
Mimas
Janus
Enceladus
Pan
Atlas
Prometheus
E
Pandora
Tethys
G
F
A
C
D
B
C
D
Epimetheus
Cordelia
Ophelia
Bianca
Cressida
Desdemona
ϵ
λ
Juliet
Portia
Uranus
Rosalind
Galle
Belinda
Despina
Naiad
Thalassa
Puck
Galatea
Larissa
Adams
Miranda
Lassell/Arago
Le Verrier
Neptune
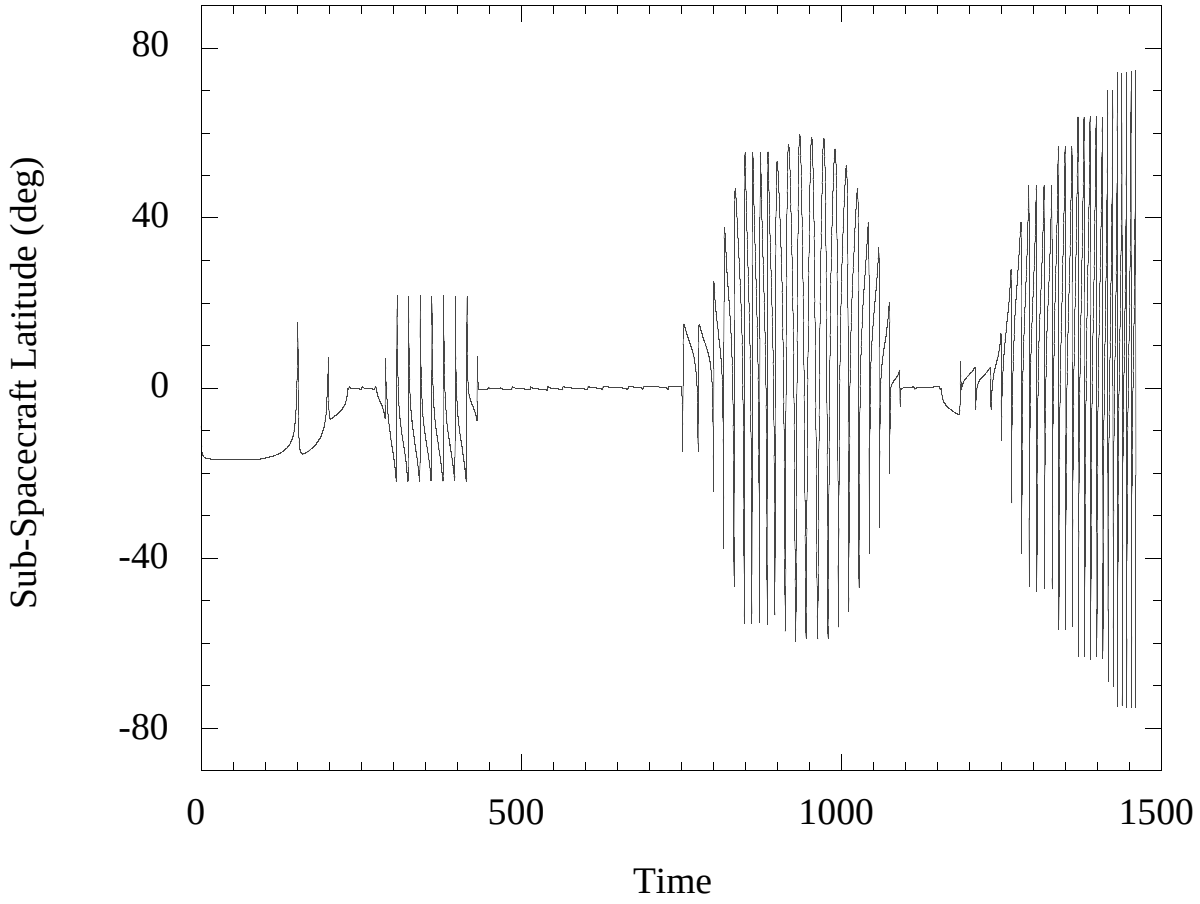
CASSINI SUB-SPACECRAFT LATITUDE
Tour T18-5